Applied and Environmental Microbiology

| Environmental Microbiology | Full-Length Text

The microbiome dynamics and interaction of endosymbiotic Symbiodiniaceae and fungi are associated with thermal bleaching susceptibility of coral holobionts

Biao Chen,[1] Yuxin Wei,[1] Kefu Yu,[1,2] Yanting Liang,[1] Xiaopeng Yu,[1] Zhiheng Liao,[1,3] Zhenjun Qin,[1] Lijia Xu,[4] Zeming Bao[1]

AUTHOR AFFILIATIONS See affiliation list on p. 21.

ABSTRACT The thermal bleaching percentage of coral holobionts shows interspecific differences under heat-stress conditions, which are closely related to the coral-associated microbiome. However, the ecological effects of community dynamics and interactions between Symbiodiniaceae and fungi on coral thermal bleaching susceptibility remain unclear. In this study, we analyzed the diversity, community structure, functions, and potential interaction of Symbiodiniaceae and fungi among 18 coral species from a high thermal bleaching risk atoll using next-generation sequencing. The results showed that heat-tolerant C3u sub-clade and *Durusdinium* dominated the Symbiodiniaceae community of corals and that there were no core amplicon sequence variants in the coral-associated fungal community. Fungal richness and the abundance of confirmed functional animal-plant pathogens were significantly positively correlated with the coral thermal bleaching percentage. Fungal indicators, including Didymellaceae, Chaetomiaceae, *Schizophyllum*, and *Colletotrichum*, were identified in corals. Each coral species had a complex Symbiodiniaceae–fungi interaction network (SFIN), which was driven by the dominant Symbiodiniaceae sub-clades. The SFINs of coral holobionts with low thermal bleaching susceptibility exhibited low complexity and high betweenness centrality. These results indicate that the extra heat tolerance of coral in Huangyan Island may be linked to the high abundance of heat-tolerant Symbiodiniaceae. Fungal communities have high interspecific flexibility, and the increase of fungal diversity and pathogen abundance was correlated with higher thermal bleaching susceptibility of corals. Moreover, fungal indicators were associated with the degrees of coral thermal bleaching susceptibility, including both high and intermediate levels. The topological properties of SFINs suggest that heat-tolerant coral have limited fungal parasitism and strong microbial network resilience.

IMPORTANCE Global warming and enhanced marine heatwaves have led to a rapid decline in coral reef ecosystems worldwide. Several studies have focused on the impact of coral-associated microbiomes on thermal bleaching susceptibility in corals; however, the ecological functions and interactions between Symbiodiniaceae and fungi remain unclear. We investigated the microbiome dynamics and potential interactions of Symbiodiniaceae and fungi among 18 coral species in Huangyan Island. Our study found that the Symbiodiniaceae community of corals was mainly composed of heat-tolerant C3u sub-clade and *Durusdinium*. The increase in fungal diversity and pathogen abundance has close associations with higher coral thermal bleaching susceptibility. We first constructed an interaction network between Symbiodiniaceae and fungi in corals, which indicated that restricting fungal parasitism and strong interaction network resilience would promote heat acclimatization of corals. Accordingly, this study provides insights into the role of microorganisms and their interaction as drivers of interspecific differences in coral thermal bleaching.

Editor Jennifer F. Biddle, University of Delaware, Lewes, Delaware, USA

Address correspondence to Kefu Yu, kefuyu@scsio.ac.cn.

The authors declare no conflict of interest.

See the funding table on p. 21.

Received 3 November 2023
Accepted 19 January 2024
Published 6 March 2024

KEYWORDS coral holobiont, microbiome dynamics, potential interaction, Symbiodiniaceae, fungi, thermal bleaching susceptibility

Coral reefs are biodiversity hotspots with the most diverse symbioses in the ocean and provide habitats for more than 30% of the marine multicellular organisms (1–3). However, global warming and its amplified marine heatwaves have led to a serious degradation of coral reef ecosystems worldwide (4–6), and global coral cover has dramatically declined by approximately 50%–80% since the 1970s (7). The exceptional marine heatwaves induced by El Niño between 2015 and 2017 directly led to 91.1% of reefs along the Great Barrier Reef (GBR) experiencing thermal bleaching (8), and coral species with staghorn and tabular shapes almost died out (9, 10). This unprecedented long-term tropical marine heatwave has caused an 89% loss of reef-building coral cover in the reefs of Kiritimati in the equatorial Pacific, which has also resulted in large-scale bleaching and high mortality of coral (6, 11). The global climate model predicts that the frequency and scale of coral thermal bleaching events will increase (12, 13) and that annual bleaching events will occur globally in coral reefs from the mid-21st century (14). Intensifying global warming and climate change have led to the collapse of the structure and ecological functions of coral reef ecosystems, resulting in irreversible regime shifts (4, 11). Interestingly, corals showed significant interspecific differences in bleaching severity and heat tolerance during heatwave events. Some coral species occurred bleached at a colony scale in low-temperature conditions (<10% of all coral bleaching), whereas colonies of other species experienced bleaching in extremely high-temperature conditions (>80% of all coral bleaching; e.g., *Pocillopora*, *Acanthastrea*, *Galaxea*, and Fungiidae), which have been found in the Red Sea and GBR (4, 15). However, the reasons for the distinct survival rates of different coral species at extremely high temperatures remain unclear.

Corals are holobionts composed of animal hosts, endosymbiotic Symbiodiniaceae, bacteria, archaea, fungi, and viruses (3, 16, 17). The difference in phenotype, genetic characteristics, transcription, and metabolism of host were closely associated with the environmental adaptability of coral species (18–21); however, coral-associated microbiome also played a crucial role in regulating the environmental tolerance of coral holobiont. Thus, the environmental adaptability of corals is regulated by both the host and its associated microbiome (3, 22, 23), which explains the interspecific differences in heat tolerance and bleaching susceptibility (24–28). The endosymbiotic Symbiodiniaceae are the primary photosymbionts of coral species that play an important role in the health and thermal adaptive potential of coral holobionts (29). Resilient and heat-tolerant Symbiodiniaceae (e.g., *Durusdinium*) can provide additional thermal tolerance to coral holobionts (30, 31). It has been found that *Platygyra ryukyuensis* and *Favites pentagona* initially changed the heat-sensitive dominant Symbiodiniaceae to heat-tolerant *Durusdinium* during long-term marine heatwave events in the El Niño core zone and improved the thermal bleaching resistance of coral holobionts (6). The biogeographic patterns and diversity of Symbiodiniaceae have been widely reported in coral reefs and communities in subtropical and tropical zones (31–36). However, studies on the potential interactions between Symbiodiniaceae and other microbes are rare, and the effects of these interactions on the thermal bleaching susceptibility of distinct coral species have not been accurately assessed. Few studies have focused on the rare symbiont biosphere and interactions between Symbiodiniaceae members. This suggests that rare symbionts will enhance the stability and resistance of coral–Symbiodiniaceae symbioses, allowing them to better respond to external disturbances (37). It has also been found that parasitic symbionts (C7 sub-clade) are inhibited by the dominant *Durusdinium trenchii* in the symbiont interaction of corals in the South China Sea (SCS) (38). In addition, fungi have diverse functions and play key roles in bioerosion, pathogens, biogeochemical cycles, and microbiome structuring in coral reef ecosystems and have the ability to exhibit numerous functions in pelagic and benthic communities (39). Although fungi are important eukaryotic microbes in the coral-associated microbiome

and are involved in phosphorus metabolism in holobionts, their diversity, ecology, evolution, and function are not well understood (3, 40, 41). Previous studies have found that fungal communities are extremely heterogeneous and phylogenetically diverse, and no biogeographical or host-specific patterns of coral-associated fungal communities have been accurately described (28, 42, 43). However, coral holobionts show greater diversity and dissimilarity in fungal communities when they exhibit tissue lesions or live in thermal environments (44, 45). The relative abundances of Saccharomycetes and Malasseziomycetes increased in thermally bleached or heat-stressed *Porites*, *Acropora*, and *Platygyra* in tropical coral reefs (28). Thus, it has been speculated that the health and adaptability of coral holobionts are affected by the fungal community and its parasitism or infection. A prime example was that of *Aspergillus* leading to *Aspergillus aspergillosis* disease and high mortality of sea fans in West India, which satisfied Koch's rule (46). Nevertheless, the link between coral-associated fungi and interspecific differences in coral heat tolerance remains unclear, and there is little information on the potential interactions between coral-associated fungi and other microbes (47, 48), especially the endosymbiotic Symbiodiniaceae, which is crucial for assessing the adaptability of coral holobionts to global warming and intensifying marine heatwaves.

Huangyan Island (HYI; 15°13′48″–15°05′24″ N, 117°40′12″–117°52′00″ E; Fig. 1a and b) is located in the eastern section of the SCS. It is an isolated atoll and one of the major components of the Zhongsha Islands. A recent study found that the highest probability of coral thermal bleaching occurred at 15–20 latitudes north and south of the Equator, based on synthesizing coral bleaching events at 3,351 sites from 81 countries (1998–2017) (49). Thus, the coral reefs of HYI will probably experience enhanced thermal bleaching and stress in the future. The result of monthly average sea surface temperature (SST; 2012–2022) analysis showed that the SST of HYI (29.3°C ± 1.3°C) was higher than those of other coral reefs at the same latitude (e.g., Xisha Island; 28.1°C ± 1.9°C), which was similar to those of coral reefs at low-latitude regions (e.g., Nansha Islands; 29.4°C ± 1.1°C; Fig. 1c). The average Symbiodiniaceae density of corals (3.12 ± 0.11 × 10^6 cells·cm^{-2}) (50, 51), coral recruitment (15.7 ± 2.2 ind·m^{-2}), and crustose coralline algae cover (42%) (52) in HYI was higher than those in other tropical coral reefs in the SCS. In addition, HYI is a submerged atoll and has strong water exchange between the outer reef slope and the lagoon (51, 53), which contributes to the overall environmental

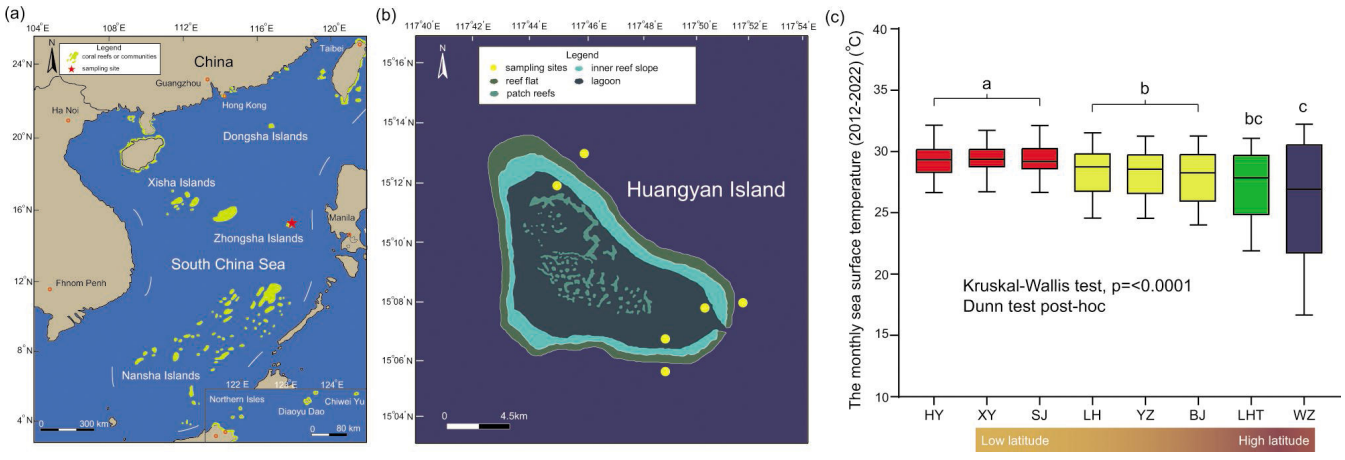

FIG 1 Study area and sampling sites. (a) Distribution of coral reefs or communities in the SCS. The red star denotes HYI; (b) physiognomy of HYI, an isolated atoll in the eastern SCS. The yellow points represent sampling sites; (c) monthly sea surface temperatures (2012–2022). Xinyi Reef (XY; 9°20′–9°21′ N, 115°54′–115°58′ E) and Sanjiao Reef (SJ; 10°10′–10°13′ N, 115°16′–115°19′ E) are located in the Nansha Islands in the low-latitude region of the SCS. Langhua Reef (LH; 16°0′–16°5′ N, 112°26′–112°35′ E), Yuzhuo Reef (YZ; 16°18′–16°21′ N, 111°57′–112°5′ E), and Beijiao (BJ; 17°06′–17°07′ N, 111°28′–111°31′ E) are distributed in the Xisha Islands in the intermediate-latitude region of the SCS. The fringe reefs of Luhuitou (LHT; 18°12′–18°13′ N, 109°28′–109°29′ E) and Weizhou Island (WZ; 21°00′–21°04′ N, 109°04′–109°08′ E) are located in the biogeographical transition zone and subtropical climate zone, respectively, both belonging to the northern part of the SCS. Different colors indicate the results of the Dunn test post-hoc analysis.

stability of HYI among the geomorphological belts. Thus, coral reefs of HYI have a thermal environment and robust ecological status, which provide a natural laboratory for exploring the effects of microbiome dynamics and interactions between Symbiodiniaceae and fungi on the heat tolerance of coral holobionts in intermediate-latitude regions with high coral thermal bleaching risk.

This study aimed to analyze the diversity and community structure of Symbiodiniaceae and fungi among 18 coral species in HYI and to evaluate the interspecific differences in microbial community flexibility. We constructed links between ecological indices (α-diversity and potential fungal pathogens abundance) of these microbial communities and coral thermal bleaching percentage in the 15–20°N regions of the SCS during the 2020 coral bleaching event (Table 1), which will assist us in explaining how distinct community dynamics of Symbiodiniaceae and fungal and pathogen abundance are linked to thermal susceptibility. Indicators of fungi and Symbiodiniaceae were also characterized in this study. Moreover, the molecular ecological network was used to explore potential interactions between dominant Symbiodiniaceae and fungi, which assisted in identifying key microbial drivers and establishing associations between the topological properties of the Symbiodiniaceae–fungi interaction network (SFIN) and coral thermal bleaching susceptibility. The results of this study will expand our knowledge of the effects of microbiome dynamics and interactions between Symbiodiniaceae and fungi on interspecific differences in coral heat tolerance in the context of global warming.

RESULTS

The coral thermal bleaching percentage and environmental characteristics

Eighteen coral species exhibited varying degrees of thermal bleaching in the 15–20°N regions of the SCS during the coral bleaching event of 2020. The thermal bleaching prevalence has weak associations with coral skeletal morphology and polyps. *Goniastrea retiformis* populations experienced the most serious thermal bleaching, the average bleaching prevalence was 94.12% (Table 1). The *Acropora nana* (87.50%), *Favites halicora* (72.73%), *Acropora anthocercis* (70.00%), *Isopora palifera* (65.00%), *Isopora cuneata* (65.00%), *Goniastrea pectinata* (61.54%), *Acropora gemmifera* (60.61%), and *Coelastrea aspera* (60.00%) also showed severe thermal bleaching (Table 1). Additionally,

TABLE 1 The coral sample information in HYI and the thermal bleaching percentage of coral species in the 15–20°N regions of the SCS during the coral bleaching event of 2020

Coral family	Genus	Species	Number of samples	Thermal bleaching percentage
Merulinidae	*Goniastrea*	*Goniastrea retiformis*	3	94.12%
Acroporidae	*Acropora*	*Acropora nana*	4	87.50%
Merulinidae	*Favites*	*Favites halicora*	6	72.73%
Acroporidae	*Acropora*	*Acropora anthocercis*	5	70.00%
Acroporidae	*Isopora*	*Isopora palifera*	6	65.00%
Acroporidae	*Isopora*	*Isopora cuneata*	3	65.00%
Merulinidae	*Goniastrea*	*Goniastrea pectinata*	5	61.54%
Acroporidae	*Acropora*	*Acropora gemmifera*	5	60.61%
Merulinidae	*Coelastrea*	*Coelastrea aspera*	3	60.00%
Agariciidae	*Leptoria*	*Leptoria phrygia*	6	59.09%
Poritidae	*Porites*	*Porites lutea*	6	54.73%
Merulinidae	*Merulina*	*Merulina ampliata*	6	50.00%
Pocilloporidae	*Pocillopora*	*Pocillopora woodjonesi*	3	47.62%
Plesiastreidae	*Plesiastrea*	*Plesiastrea versipora*	4	43.75%
Merulinidae	*Dipsastraea*	*Dipsastraea speciosa*	3	33.33%
Pocilloporidae	*Pocillopora*	*Pocillopora verrucosa*	5	17.84%
Merulinidae	*Hydnophora*	*Hydnophora exesa*	5	5.00%
Fungiidae	*Fungia*	*Lobactis scutaria*	3	2.00%

Leptoria phrygia (59.09%), *Porites lutea* (54.73%), *Merulina ampliata* (50.00%), *Pocillopora woodjonesi* (47.62%), *Plesiastrea versipora* (43.75%), and *Dipsastraea speciosa* (33.33%) suffered intermediated thermal bleaching during the coral bleaching event of 2020. Nevertheless, *Pocillopora verrucosa* (17.84%), *Hydnophora exesa* (5.00%), and *Lobactis scutaria* (2.00%) exhibited lower thermal bleaching susceptibility than other coral species, with thermal bleaching percentages below 20% (Table 1).

Statistical analysis of the environmental parameters revealed that no significant differences were observed in the temperature (°C), salinity (PSU), DO (mg/L), pH, and turbidity (FNU) between the outer reef slope and the lagoon in HYI (Fig. 2; Table. S1). Although the concentration of SiO_3^{2-}, PO_4^{3-}, NH_4^+, and NO^{3-} of seawater in the lagoon was lower than that in the outer reef slope in HYI, there was also no significant difference of nutrients across the geomorphological belts. This phenomenon can be attributed to the close association of HYI with submerged atoll and strong water exchange.

The diversity of Symbiodiniaceae and fungi

After blasting and filtering the reads, 5,251,966 Symbiodiniaceae ITS2 reads were obtained. *Cladocopium*, *Durusdinium*, and *Gerakladium* were identified in the 18 HYI coral species based on ITS2 sequence analysis after quality control (retaining ITS2 variants present with at least 1% abundance in at least one sample). At the sub-clade taxonomic level, 45 Symbiodiniaceae sub-clades were identified, of which the three genera were *Cladocopium* (*n* = 39), *Durusdinium* (*n* = 5), and *Gerakladium* (*n* = 1). In addition, 1,217 Symbiodiniaceae ASVs were identified after filtering and subsampling, which were used for Chao1 richness index statistics and to reduce the distraction of intragenomic variation. For the fungal community, the 2,142,129 sequences were aligned to fungi and

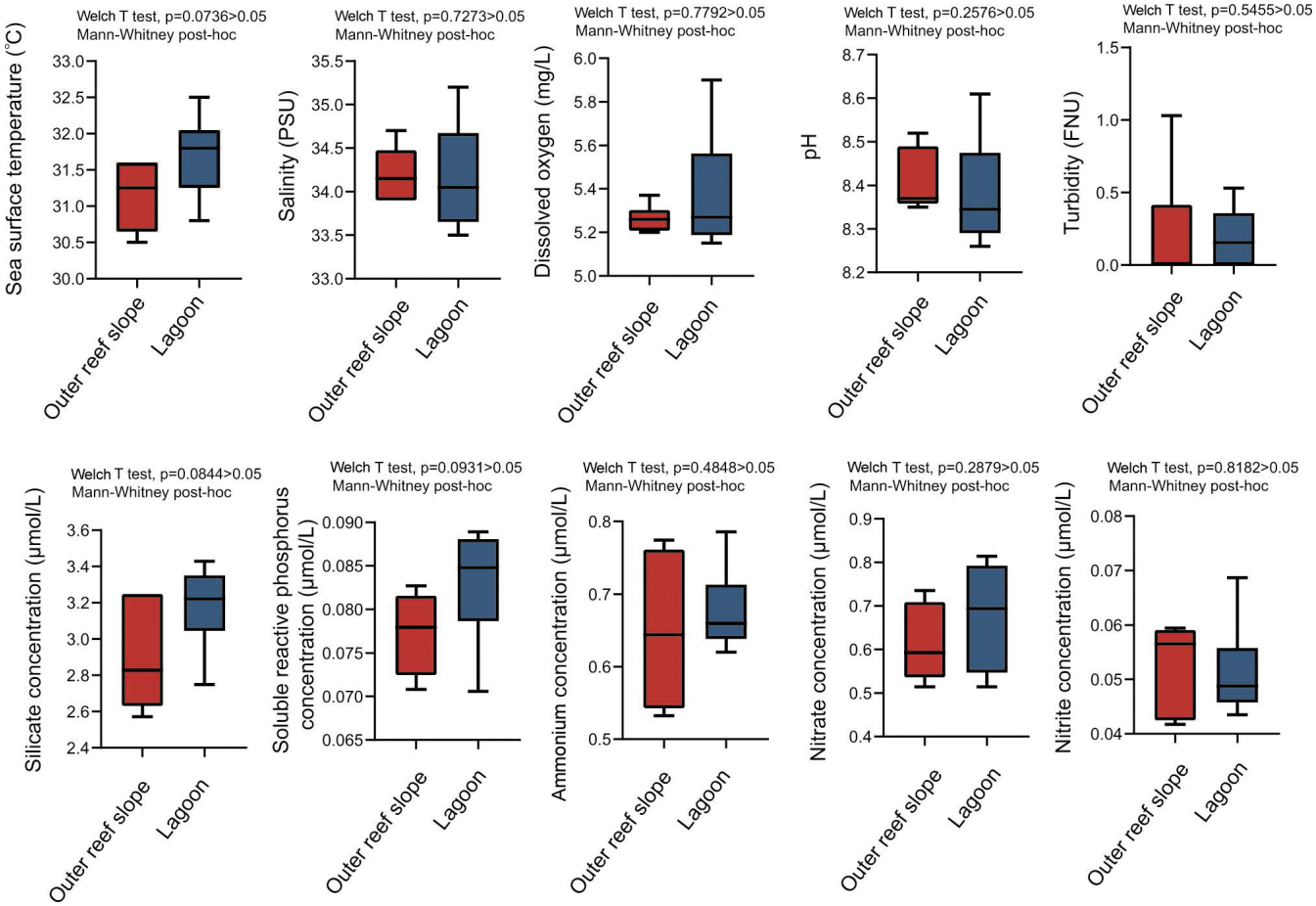

FIG 2 The statistical result of environmental factors between outer reef slope and lagoon in of coral reef in Huangyan Island.

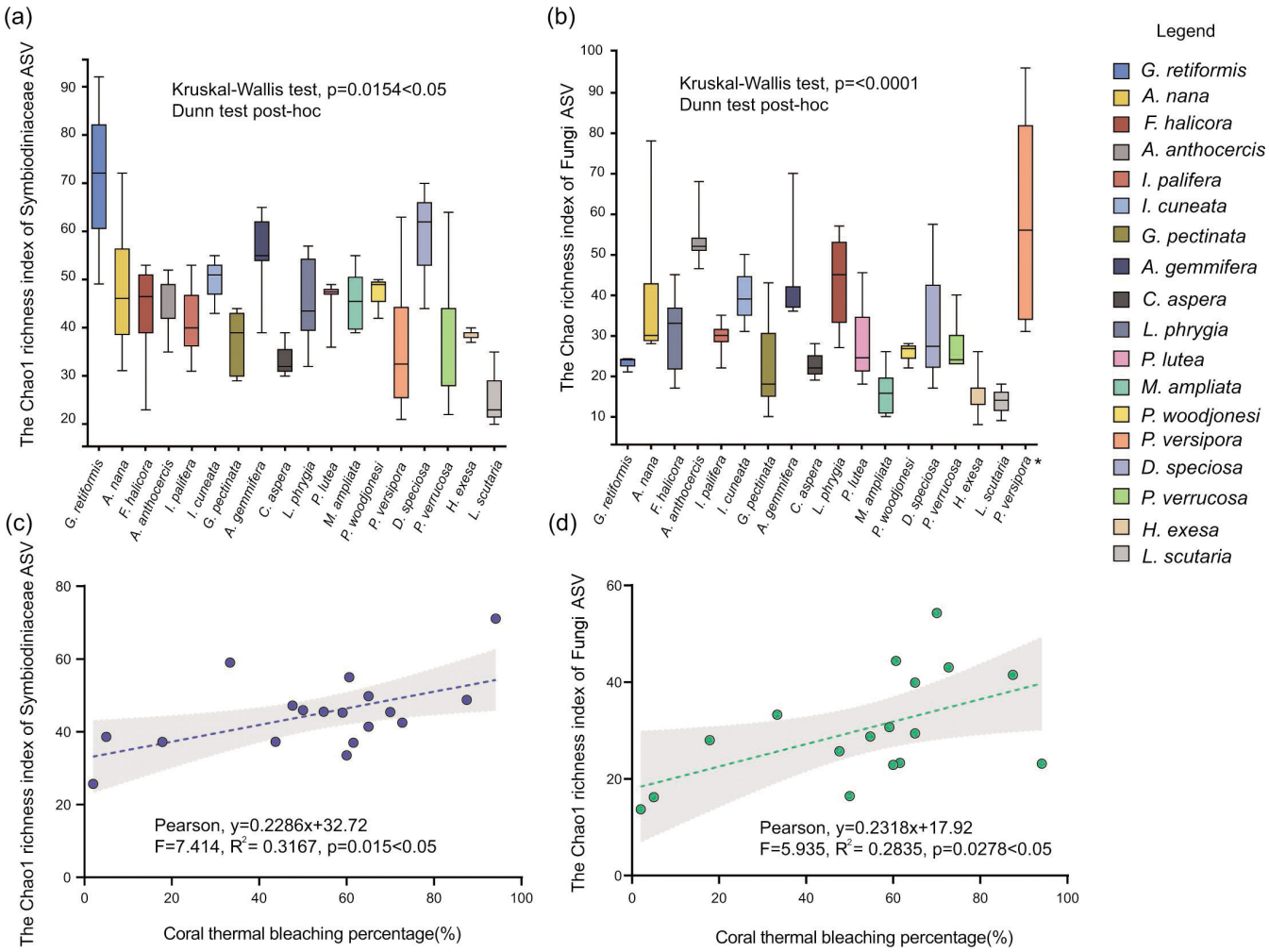

FIG 3 The α-diversity of Symbiodiniaceae and fungi of 18 coral species in HYI. The Chao1 richness index of (a) Symbiodiniaceae and (b) fungi of 18 species of corals in HYI; the correlation between the Chao1 richness index of (c) Symbiodiniaceae/ (d) fungi and the degree of coral susceptibility. The asterisk denotes abnormally high value of Chao1 richness index in *P. verispora*.

clustered as ASVs after quality control and data set subsampling; there were 6 phyla, 26 classes, 55 orders, 119 families, 178 genera, 236 species, and 1,881 ASVs identified in 18 HYI coral species. In addition, there were significant differences in the Chao1 richness index of Symbiodiniaceae (Kruskal–Wallis test, $P = 0.0154 < .05$; Fig. 3a) and fungi (Kruskal–Wallis test, $P < 0.0001$; Fig. 3b) among HYI coral holobionts. The simple linear regression (SLR) analysis revealed that the coral thermal bleaching percentage was significantly and positively associated with the richness of Symbiodiniaceae (Pearson, $F = 7.414$, $R^2 = 0.3167$, $P = 0.015 < .05$; Fig. 3c). Nevertheless, there was a significantly positive correlation between Chao1 richness index of fungi and thermal bleaching percentage of coral holobiont (Pearson, $F = 5.935$, $R^2 = 0.2835$, $P = 0.0278 < .05$; Fig. 3d).

The community structure of Symbiodiniaceae

The Symbiodiniaceae community of coral in HYI was mainly dominated by *Cladocopium* (91.5% ± 17.1%) and *Durusdinium* (5.3% ± 16.8%). There were 21 dominant Symbiodiniaceae sub-clades (the relative abundance was >5% in at least one sample; Fig. 4a). The C3u sub-clade dominated the Symbiodiniaceae community of corals in HYI (42.7% ± 32.8%; Fig. 4b), which had a high relative abundance in 13 of the 18 coral species. However, the Symbiodiniaceae community of *G. retiformis* was dominated by C1# (70.3% ± 12.7%), C1 (8.2% ± 13.1%), and D1 (4.7% ± 6.0%), and the relative abundance of

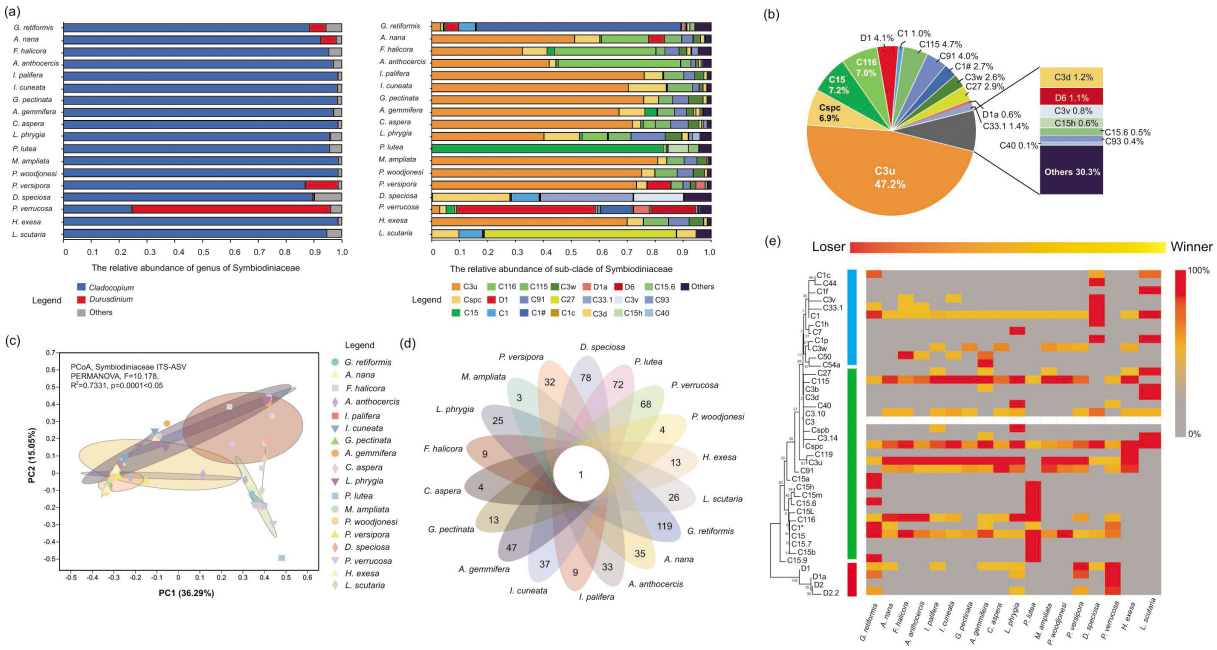

FIG 4 The community structure of Symbiodiniaceae among eighteen18 coral species in HYI in the SCS. (a) Relative abundance of genus and sub-clade of Symbiodiniaceae in 18 coral species in HYI; (b) community composition of Symbiodiniaceae of corals in HYI; (c) principal co-ordinates analysis (PCoA) of Bray–Curtis distances of Symbiodiniaceae ASV compositions associated with 18 coral species. Ellipses denote significant differences among 18 coral species [permutational multivariate analysis of variance (PERMANOVA)]; (d) the Venn diagram visualization for ubiquitous and specific Symbiodiniaceae ASV of 18 coral species; (e) abundance and enrichment characteristics of Symbiodiniaceae bio-indicator of 18 coral species in HYI based on ASV data set analyses. The blues and green rectangles denote thermally sensitive and tolerant Symbiodiniaceae sub-clades of *Cladocopium*, respectively, based on the results of phylogenetic analysis. The red rectangle represents heat-tolerant Symbiodiniaceae sub-clades of *Durusdinium*.

C3u was 3.2% ± 2.1%. In addition, *D. speciosa* had diverse dominant Symbiodiniaceae sub-clades: C33.1 (33.1% ± 1.0%), Cspc (27.8% ± 0.6%), C3v (17.8% ± 2.0%), and C1 (9.8% ± 1.0%) contributed high relative abundance to the symbiont community. It is worth noting that the relative abundance of *Durusdinium* was higher than that of *Cladocopium* in *Pocillopora verrucosa*, D1 (49.3% ± 18.0%) and D6 (15.6% ± 10.3%) were dominant in the Symbiodiniaceae community, but C1# (10.8% ± 18.1%) had the highest relative abundance in *Cladocopium*. Moreover, the C27 (68.8% ± 9.7%) and C15 (82.4% ± 5.5%) were predominant in the Symbiodiniaceae communities of *L. scutaria* and *P. lutea*, respectively.

The results of PCoA showed that there were significant differences in Symbiodiniaceae community structure among coral species in HYI (permutational multivariate analysis of variance; PERMANOVA, F = 10.178, R^2 = 0.7331, P = 0.0001 < .05), and the 51.3% total variation in the Symbiodiniaceae community was explained by interspecific differences (Fig. 4c). The Venn diagram visualization revealed that the core symbiont microbiome had only one Symbiodiniaceae ASV (ASV 506), which aligned with the variant of the C3u sub-clade and lived in all HYI coral species (Fig. 4d). Moreover, the IndicSpecies test-based ASV data set analyses identified 45 indicators of the Symbiodiniaceae sub-clade among 18 coral species (Fig. 4e). The heat-sensitive C1 sub-clade and heat-tolerant Cspc, C3u, C91, C15, and C116 sub-clades were ubiquitous among coral species that have distinct thermal bleaching susceptibilities. It is worth noting that *Durusdinium* spp. do not show enrichment characteristics in all strong heat-tolerant coral species (e.g., *P. woodjonesi*, *H. exesa*, and *L. scutaria*) except *P. verrucosa*; these coral holobionts preferred to have symbioses with potential thermal-sensitive (e.g., C1 and *L. scutaria*) or tolerant *Cladocopium* (e.g., C115, C3u, Cspc, C119, C91, and *L. scutaria*; C115, C3u, and *P. woodjonesi*).

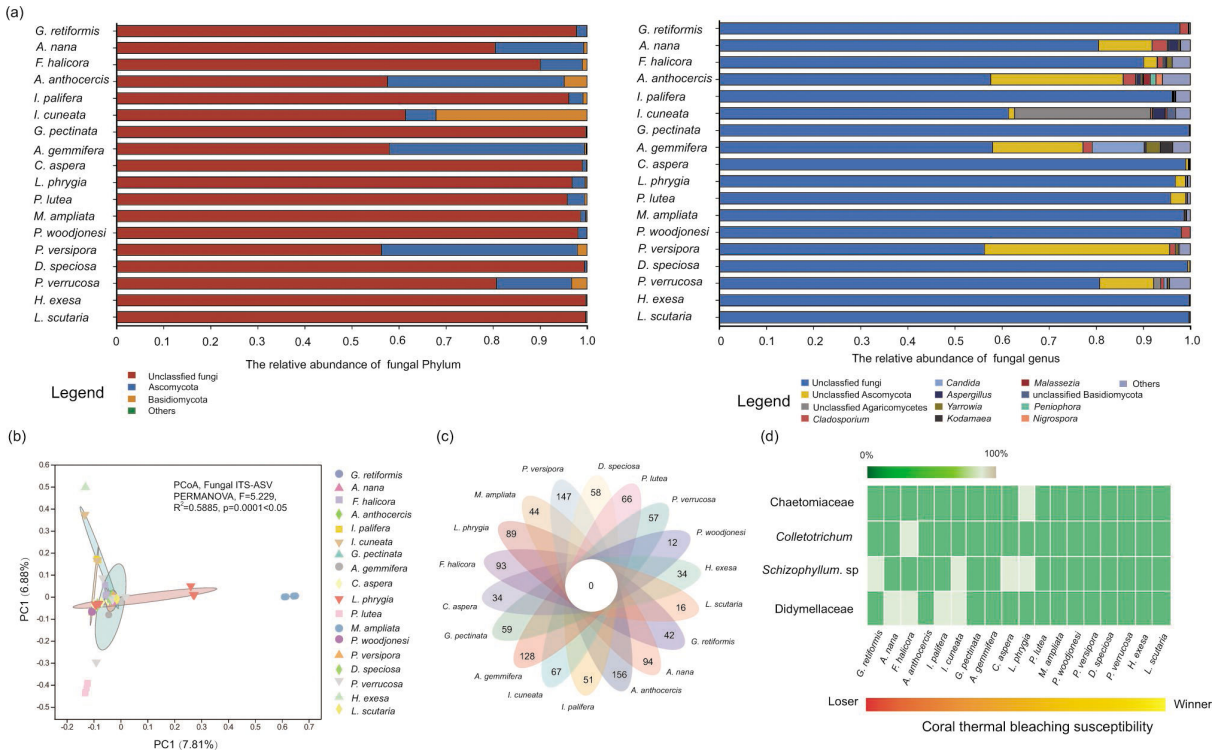

FIG 5 The community structure of fungi among 18 coral species in HYI in the SCS. (a) Fungal community composition for phylum, genus, and ASV levels of 18 coral species in HYI; (b) PCoA of Bray–Curtis distances of fungal compositions associated with 18 coral species. Ellipses denote significant differences among distinct coral species (PERMANOVA); (c) Venn diagram visualization for ubiquitous and specific fungal ASV of 18 coral species; (d) Abundance and enrichment characteristics of fungal bio-indicator of 18 coral species in HYI.

The community structure of fungi

At the phylum level, the fungal community composition of coral holobionts in HYI was dominated by Ascomycota (10.4% ± 14.7%) and Basidiomycota (2.6% ± 7.5%), and a high abundance of unclassified fungi was identified in 18 coral species (87.0% ± 16.8%; Fig. 5a). Thus, corals in HYI have a stable community composition of fungi at the phylum level. In addition, the corals in HYI were mainly colonized by *Cladosporium* (0.9% ± 1.0%), *Candida* (0.7% ± 2.6%), *Aspergillus* (0.4% ± 0.7%), *Yarrowia* (0.4% ± 0.7%), *Kodamaea* (0.2% ± 0.6%), *Malassezia* (0.1% ± 0.4%), *Peniophora* (0.1% ± 0.3%), and *Nigrospora* (0.1% ± 0.3%) at the genus level, and the relative abundance of these fungal genera was >1% in at last one coral species. The mycobiome of coral also had abundant unclassified fungal taxa at the genus level, such as unclassified fungi (86.9% ± 16.8%), Ascomycota (6.7% ± 11.3%), Agaricomycetes (1.7% ± 6.8%), and Basidiomycota (0.1% ± 0.4%; Fig. 5a). However, the PCoA identified that the community structure of fungi was highly flexible among the distinct coral species (Fig. 5b). The results of the PERMANOVA test showed that there were significant differences in the fungal community structure among distinct coral species in HYI (PERMANOVA, F = 5.299, R^2 = 0.5885, P = 0.0001 < .05). In addition, the Venn diagram visualization showed that there was no core fungal ASV present in all coral species and >80% of the samples. This suggests that the fungal community of corals in HYI has high variation and flexibility (Fig. 5c). Moreover, the IndicSpecies test found that Didymellaceae (indicator test, P = 0.043 < .05), *Schizophyllum* (indicator test, P = 0.035 < .05), *Colletotrichum* (indicator test, P = 0.040 < .05), and Chaetomiaceae (indicator test, P = 0.017 < .05) were indicators of distinct coral species in HYI. It is worth noting that Didymellaceae (0%–60.3%) and *Schizophyllum* (0%–47.1%) exhibited a higher relative abundance in coral species with high thermal bleaching susceptibility and *Colletotrichum* (relative abundance: >90%)

and Chaetomiaceae (relative abundance: >90%) displayed relatively higher levels in *F. halicora* and *L. phrygia*, which demonstrate intermediate heat tolerance (Fig. 5d; Table.S2). However, the abundance of these four fungal indicators did not show any associations with coral species with stronger thermal adaptability.

The functional traits of the fungal community

The results of the FUNGuild analysis showed that the ecological functions of 96% of fungi in the corals in HYI were unknown (Fig. 6a), which was consistent with the result of fungal community composition. The predictable ecological functional fungal community (4%) of corals in HYI was mainly colonized by undefined saprotrophs (US; 36.7% ± 22.1%) and animal pathogen–endophyte–lichen parasite–plant pathogen–wood saprotroph (AELPW; 25.1% ± 27.6%) fungi, which were distributed in almost all coral species, except for heat-tolerant *L. scutaria* and *H. exesa* (Fig. 6a). The known functional fungal community of *L. scutaria* was dominated by animal pathogen–endophyte–epiphyte–plant pathogen-undefined saprotroph (AEEPS; 99.4% ± 2.3%) fungi, and animal pathogen–plant pathogen-undefined saprotroph fungi (AEEPS; 72.1% ± 5.7%) had the highest relative abundance in the fungal community of *H. exesa* (Fig. 6a). In addition, the predictable functional fungal communities of HYI corals were also colonized by plant pathogen (PP; 4.8% ± 7.2%), animal pathogen-undefined saprotroph (AS; 2.4% ± 4.1%), animal pathogen-plant pathogen-undefined saprotroph (APS; 5.6% ± 17.0%), wood saprotroph (WS; 3.0% ± 4.4%), plant pathogen-wood saprotroph (PW; 1.2%

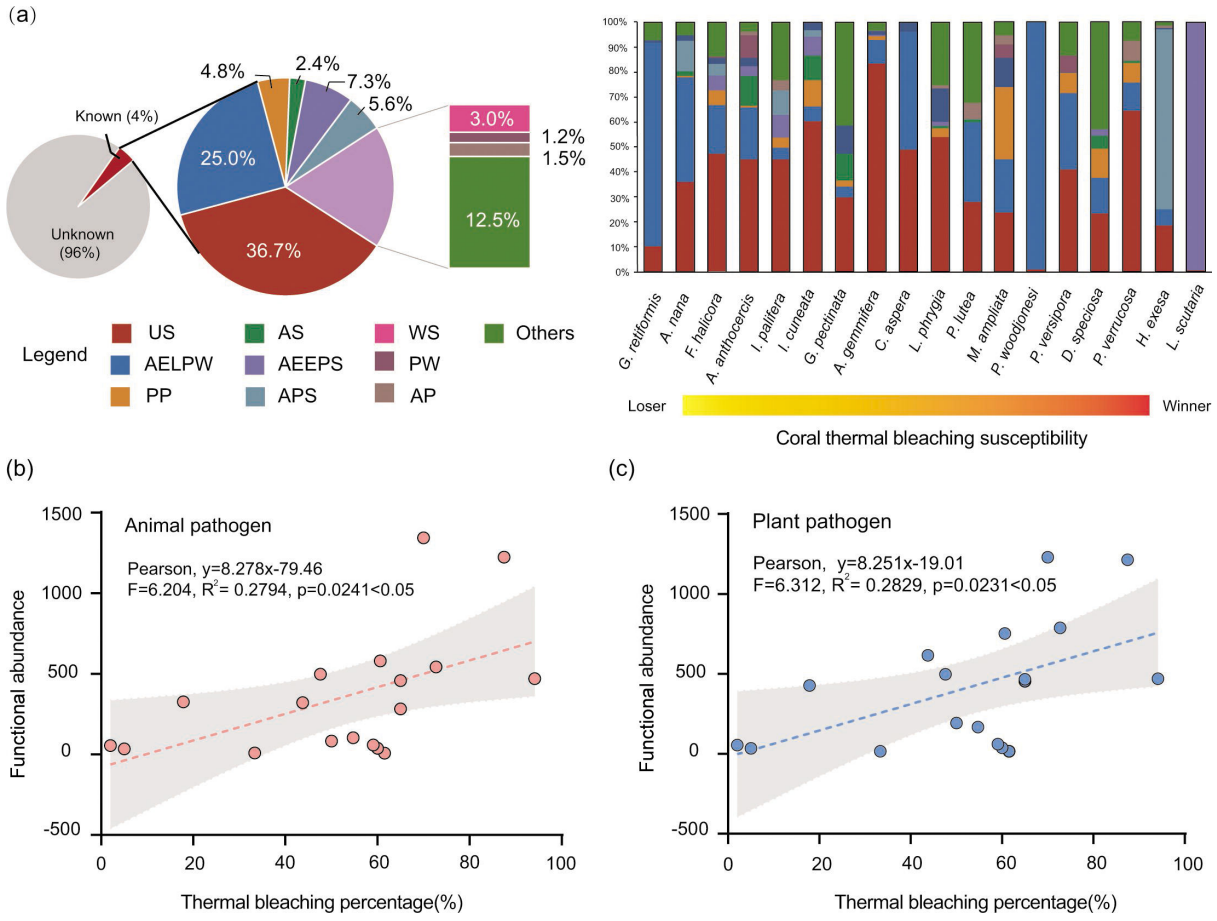

FIG 6 The relationship between the relative abundance of fungal pathogen function traits and coral thermal bleaching susceptibility. (a) Composition of fungi function group among coral species in HYI. The relative abundance of US, AELPW, PP, AS, AEEPS, APS, WS, PW, and AP was more than 1%; (b) There was a significantly positive correlation between the abundance of animal pathogen of fungi and coral thermal bleaching percentage (%). (c) There was a significantly positive association between the coral thermal bleaching percentage (%) and the abundance of fungal plant pathogen.

± 2.8%), and animal pathogen (AW; 1.5% ± 2.5%) fungi, and the relative abundance of these functional groups was >1% (Fig. 6a). Notably, fungal parasite-associated fungi were rare in the corals in HYI, and the total relative abundance of this functional fungal group was only 1.2%.

The results of SLR showed that the abundance of functional traits of animal pathogens in the fungal community had a significantly positive correlation with coral thermal bleaching percentage (Pearson, F = 6.204, R^2 = 0.2794, P = 0.0241 < .05; Fig. 6b). In addition, the heat adaptability and acclimatization of coral holobionts also related with the reduction of plant-pathogenic fungi, because the thermal bleaching percentage of coral holobionts had a significantly positive association with the abundance of functional profiles of plant pathogens in the fungal community (Pearson, F = 6.312, R^2 = 0.2829, P = 0.0231 < .05; Fig. 6c). Thus, an increase in the abundance of both animal- and plant-pathogenic fungi has closed associations with the increases of the thermal bleaching susceptibility of coral holobionts.

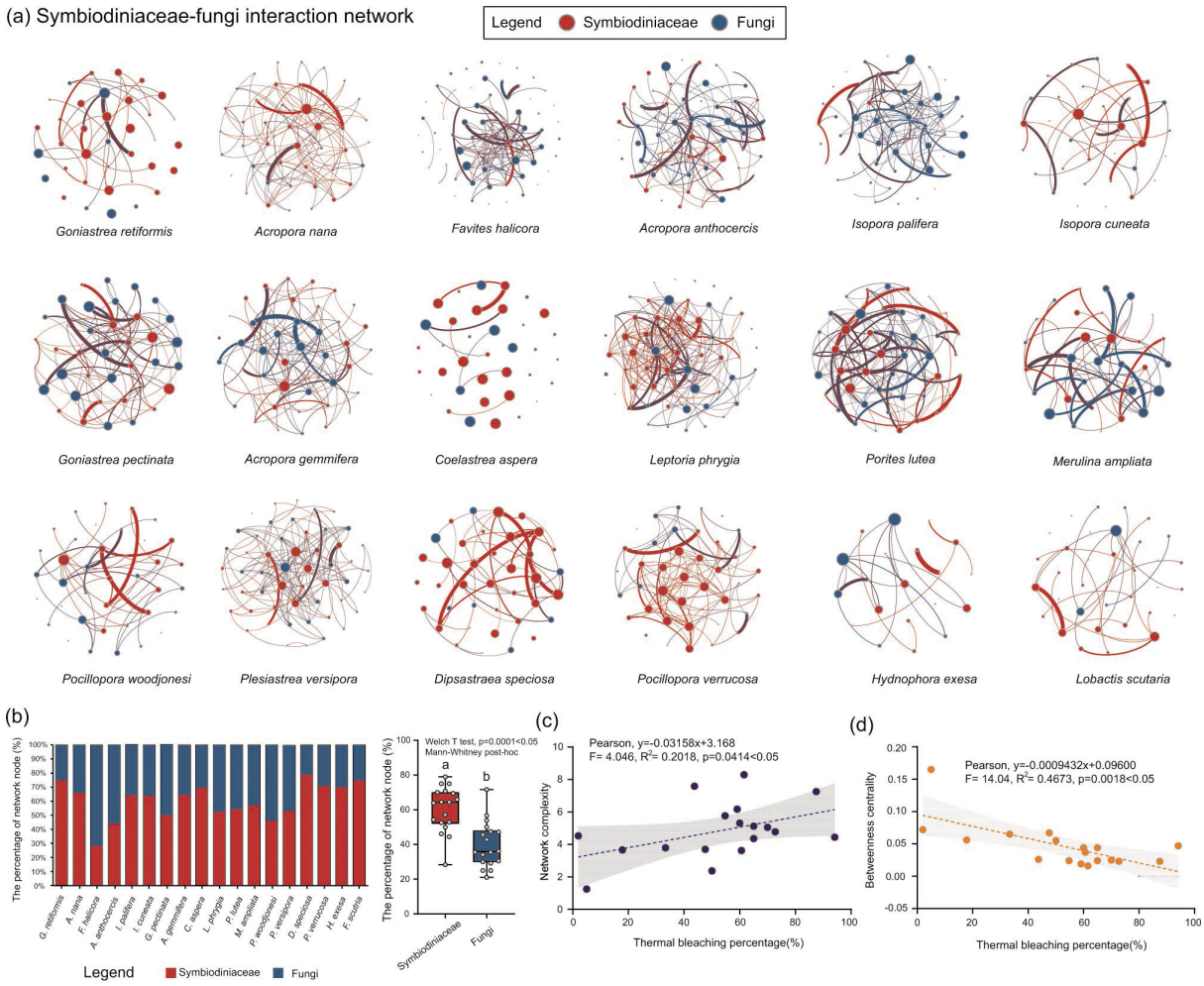

FIG 7 The correlation between the topological features of SFIN and coral bleaching susceptibility in HYI. (a) Molecular ecological interaction network of Symbiodiniaceae and fungi for 18 coral species in HYI, with co-occurrence relationships marked by edges of the network. Potential interactions of Symbiodiniaceae are denoted by red, the relationships among fungi in blue, and the co-occurrence association between Symbiodiniaceae and fungi in brown. (b) Percentage of network node for Symbiodiniaceae and fungi. (c) Correlation between complexity of SFIN and coral thermal bleaching percentage (%). (d) Relationship between betweenness centrality of SFIN and coral thermal bleaching percentage (%).

The interaction and complexity of the microbiota of Symbiodiniaceae and fungi

The results of molecular ecological network analysis (MENA) showed that there was a complexed potential interaction between dominant Symbiodiniaceae sub-clades (relative abundance > 5%) and fungi among distinct coral species (Fig. 7a). The average percentage of network node of Symbiodiniaceae was 60.2% ± 13.0% (ranging from 28.3% to 75.0%), which was significantly higher than those of fungi (39.8% ± 13.1%, ranging from 21.1% to 71.6%) in the SFIN of coral holobiont in HYI (Welch *t*-test, P = 0.0001 < .05; Fig. 7b). Symbiodiniaceae had the highest relative abundance of nodes in the SFIN of *G. retiformis*, whereas the highest percentage of fungal nodes was found in the SFIN of *F. halicora*. Therefore, the dominant Symbiodiniaceae sub-clades contributed more than fungi to the SFIN construction of the coral holobionts in HYI.

The SFIN patterns varied greatly among different coral species, as indicated by the multiple topological feature indices of the 18 networks. The total number of nodes ranged from 20 to 67, and the total number of links ranged from 25 to 320 (Table 2). In addition, there were differences in the average degree, network diameter, network centralization, average path length, clustering coefficient, and modularity of SFIN among the 18 coral species in HYI. The SFIN of *C. aspera* and *L. phrygia* had the weakest and strongest relationships among nodes, respectively. The average degree of SFIN of *C. aspera* was 0.144, whereas that of *L. phrygia* was 6.169 (Table 2), and the thermal bleaching susceptibilities of these two coral species were similar. In addition, coral species with distinct thermal bleaching tolerances had large scales of SFINs (ranging from 3 to 7; Table 2), and the SFIN diameter of *L. scutaria* with strong heat tolerance was equal to that of *A. gemmifera* with high thermal bleaching susceptibility. Regarding centralization and average path length, the SFIN of coral species with intermediate thermal bleaching susceptibility had the maximum and minimum of these topology parameters (e.g., *Coelastrea aspera*, *Favites halicora*, and *D. speciosa*). The modularity of the SFIN for coral species ranged from 0.342 to 0.800 in HYI, and the heat-sensitive *A. anthocercis* had the highest modularity (Table 2). Notably, SFIN complexity was significantly and positively correlated with coral thermal bleaching percentage (Pearson, F = 4.046, R^2 = 0.2018, P = 0.0414 < .05; Fig. 7c). Nevertheless, there was a significantly negative association between the betweenness centrality of SFIN and coral thermal bleaching percentage (Pearson, F = 14.04, R^2 = 0.4673, P = 0.0018 < .05; Fig. 7d). Thus, the coral thermal bleaching susceptibility is closely related to the complexity and betweenness centrality of SFIN.

DISCUSSION

The heat-tolerant C3u sub-clade and *Durusdinium* may provide extra thermal acclimation to coral holobionts

The endosymbiotic Symbiodiniaceae communities of coral holobionts in the HYI are dominated by *Cladocopium* and *Durusdinium*. This is consistent with the symbiont composition of corals in the Indo-Pacific regions (29, 34, 35, 54, 55). Although HYI has an approximate latitude with the Xisha Islands in the intermediate latitudes of the SCS, the average monthly SST of HYI is not significantly different from those of low-latitude regions with serious heat stress (Fig. 1c) (35, 50, 51). It is worth noting that heat-tolerant C3u contributed the highest relative abundance to *Cladocopium* in the Symbiodiniaceae communities of HYI and was consistently sustained as a core symbiont in 18 coral species (Fig. 4a), suggesting that the high abundance and stable presence of C3u may associate with lower thermal bleaching susceptibility of coral holobiont in HYI. Previous studies have found that the Symbiodiniaceae communities of *Acropora*, *Fungia*, *Platygyra*, *Symphyllia*, *Favites*, *Goniastrea*, and *Pavona* were dominated by C3u and *D. trenchii* (D1–4 sub-clades) in hot coral reefs in the Andaman Sea in the northeastern Indian Ocean, which is a part of a massive warm water zone encompassing Southeast Asia, Indonesia, and northern Australia. The abundance of C3u was higher than that of *D. trenchii* in

TABLE 2 The topological features of Symbiodiniaceae–fungi interaction network for 18 species of coral in HYI

Species	Number of nodes	Number of edges	Average degree	Network diameter	Network centralization	Characteristic path length	Clustering coefficient	Modularity	Betweenness centrality	Complexity
Goniastrea retiformis	36	160	1.611	5	0.215	2.603	0.808	0.465	0.047	4.444
Acropora nana	44	319	4.818	4	0.207	1.971	0.741	0.586	0.023	7.250
Favites halicora	67	320	2.866	7	0.433	2.518	0.575	0.659	0.023	4.776
Acropora anthocercis	63	318	3.619	5	0.315	2.509	0.572	0.8	0.025	5.048
Isopora palifera	58	297	4.662	6	0.385	2.319	0.635	0.741	0.024	5.121
Isopora cuneata	36	157	1.778	7	0.316	2.487	0.783	0.73	0.044	4.361
Goniastrea pectinata	38	315	5.158	3	0.269	1.582	0.674	0.69	0.016	8.289
Acropora gemmifera	45	163	4.622	6	0.256	2.588	0.621	0.627	0.037	3.622
Coelastrea aspera	36	191	0.444	4	0.192	1.58	0.86	0.342	0.044	5.306
Leptoria phrygia	59	364	6.169	5	0.351	2.093	0.526	0.452	0.019	6.169
Porites lutea	46	265	5.87	6	0.453	2.064	0.559	0.684	0.024	5.761
Merulina ampliata	35	83	3.257	7	0.164	2.802	0.349	0.699	0.055	2.371
Pocillopora woodjonesi	39	144	1.897	3	0.15	1.662	0.835	0.666	0.067	3.692
Plesiastrea versipora	53	402	5.019	5	0.296	2.319	0.818	0.645	0.026	7.585
Dipsastraea speciosa	38	144	2.105	8	0.107	3.254	0.79	0.543	0.065	3.789
Pocillopora verrucosa	41	150	4.829	7	0.238	2.524	0.607	0.791	0.056	3.659
Hydnophora exesa	20	25	1.9	4	0.361	2.044	0.523	0.647	0.165	1.250
Lobactis scutaria	36	163	1.389	7	0.25	2.534	0.773	0.453	0.072	4.528

offshore reefs with increasing seawater transparency (31, 56). In addition, the C3u also contributed high relative abundance (29.4% ± 21.2%) in the Symbiodiniaceae community composition of corals in the southern SCS that was controlled by long-term thermal stress (35, 57, 58), and about 2/3 of coral species was colonized by C3u across outer reef slopes and lagoons in these regions (50, 59). Phylogenetic and ecological studies have found that the C3u sub-clade was derived from C3 after the Late Miocene or Early Pliocene based on ITS2 gene marker (Fig. 4e), making it a potential recent heat-tolerant ancestor of *Cladocopium* (35, 60). The relative abundance of C3u sub-clade in coral holobionts has significantly positive associations with SST and photosynthetically active radiation across 19 latitudes of the SCS (PAR) (35).

Interestingly, heat-tolerant C3u and *Durusdinium* (D1 and D6) have the ability to dominate the Symbiodiniaceae community of the same coral samples or species in HYI and other low-latitude coral reefs (Fig. 4a), for example, *Echinopora*, *Pocillopora*, and *Diploastrea* have symbioses with C3u and D1 in the Perhentian Islands and Redang Islands in Malaysia (61). This symbiotic characteristic has also been identified in corals from the Gulf of Thailand (e.g., *Platygyra daedalea*) and the Philippine Archipelago (62, 63), suggesting that corals prefer to establish symbioses with heat-tolerant C3u and *Durusdinium* at the same time in long-term and stable thermal stress environment. It has been generally recognized that *Durusdinium* is a heat-tolerant Symbiodiniaceae that can provide 1.0°C–2.0°C of additional thermal tolerance to the coral holobiont (3, 29, 56, 64). A recent study found that coral holobionts shifted the dominant symbiont of the Symbiodiniaceae community from *Cladocopium* to *Durusdinium* in the central equatorial Pacific Ocean during the 2015–2016 El Niño event. This enhanced the survival and resilience of corals during long-term marine heatwaves (6). However, calcification and photosynthetic efficiency in coral hosts harboring *Durusdinium* are greatly reduced compared with those of corals harboring native *Cladocopium* (56, 65). Thus, the coral has symbioses with heat-tolerant C3u and *Durusdinium*, which may assist the coral to improve heat resistance potential and avoid the negative impact of symbioses on the growth and health of the holobiont. It has been found that *P. verrucosa*, *G. retiformis*, and *A. nana* had higher live coral cover (9.16%, 3.69%, and 0.89%, respectively) and dominance (0.086, 0.032, and 0.032, respectively) than other coral species in thermal HYI (53, 66), which simultaneously established symbioses with heat-tolerant C3u and *Durusdinium*. Nevertheless, corals also have the ability to establish symbioses with diverse sub-clades of *Cladocopium* or have specific symbioses with only one *Cladocopium* taxon (Fig. 4a). This leads to significant interspecific differences in Symbiodiniaceae community structure among coral species in HYI. It was worth noting that these Symbiodiniaceae sub-clades were mostly derived from C3 (Cspc, C27, and C91) or C15 (C116 and C115) (31, 35, 60), which may have inherited thermal adaptability from a potential heat-tolerant ancestor. It has been widely reported that C27- *L. scutaria* and C15- *P. lutea* symbioses have a low thermal bleaching susceptibility (4, 9, 67–69). Accordingly, the Symbiodiniaceae community of coral in HYI was primarily characterized by the prevalence of heat-tolerant sub-clades of *Cladocopium* and *Durusdinium*, which may potentially equip the corals in HYI with increased thermal tolerance, enabling them to respond to heat stress condition akin to those experienced in low-latitude regions.

The increase of fungal diversity and pathogen abundance was associated with higher thermal bleaching susceptibility of corals

This study found that the fungal alpha diversity and the richness of unique fungal ASVs have a significantly positive correlation with thermal bleaching percentage of corals in HYI, which suggests that an increase in fungal diversity and richness was associated with the higher coral thermal bleaching susceptibility. Fungal diversity is closely associated with environmental stress levels, such as SST, depth, nutrient concentration, and disease (39, 70, 71). For example, the fungal diversity of *Acropora loripes* increased with water depth and available nutrients in the Gulf of Aqaba, and the fungal diversity of lesioned coral colonies was higher than that of healthy coral colonies (45). In addition, Amend

et al. (44) showed that the fungal community of *Acropora hyacinthus* in warmer habitats contained more phylogenetic diversity than that of *A. hyacinthus* in colder habitats of Ofu Island in American Samoa (44). Notably, metagenomic analyses have revealed fungal proliferation and increased zoosporic members under thermal or environmental stress (71–73). Thus, this study suggests that the diversity and abundance of potentially opportunistic or pathogenic fungi have closed associations with interspecific difference of thermal bleaching susceptibility in coral. Additionally, the activity of pathogenic fungi has a negative ecological impact on corals, Symbiodiniaceae, and endolithic algae in heat-stressed environments. The results of the FUNGuild analysis showed that an increase in the abundance of animal and plant pathogenic fungi was related with higher coral thermal bleaching susceptibility, and heat-tolerant coral species (e.g., *L. scutaria*, *H. exesa*, and *P. woodjonesi*) have a low functional abundance and diversity of pathogenic fungi (Fig. 6b and c). Nevertheless, a substantial proportion of fungi taxa in corals of HYI remained unclassified (87.0% ± 16.8%), and only 4% of fungal ecological functions has been identified. Hence, the potentially positive or negative impact of these unidentified mycobiome on heath state and thermal tolerance susceptibility of coral holobiont need to be further studied.

Notably, there were no core fungal ASVs among the 18 coral species in HYI, suggesting that the fungal communities of corals have high flexibility and interspecific heterogeneity. Coral holobionts share the same fungal taxa at phylum and class levels globally, for example, ascomycetes have been identified in almost all ecological and microbiological studies on coral–associated fungi (28, 39, 43, 45, 73–75), and Sordariomycetes, Dothideomycetes, Eurotiomycetes, and Saccharomycetes are widely distributed across coral reefs worldwide (42, 71, 76). However, the core fungal taxa were rare at the species, operational taxonomic units (OTUs), and ASV levels, even for one coral species in the same region. Only 11 core fungal OTUs from four classes have been identified in 90% of *A. hyacinthus* colonies ($n = 36$) based on 454 DNA amplicon sequences in the Red Sea (44). The numbers of core fungal ASVs or OTUs of corals were much less than those of bacteria and Symbiodiniaceae (Fig. 5d) (77–79), which suggests that phylogenetic association and coevolution between corals and fungi was limited, and the flexibility of the fungal community might be higher than that of the bacterial community in coral holobionts. However, the intragenomic polymorphism of eukaryotic cell may also play a role in the variability and flexibility of fungal community. Interestingly, changes in fungal diversity were similar to those of bacterial diversity; they all had positive associations with global or local environmental stress level of coral. Thermal or other stress factors (e.g., low pH, human interference, and algal contact) tend to increase bacterial alpha diversity (80–85), because the coral holobiont is an open microbial system (17, 86), and microbial invasion and heat stress disrupt the microbiome function and increase the number of microbes not typically resident in corals (85, 87). Additionally, it has been found that the fungi skewed toward having a negative impact on the heath state of coral holobionts under the environment stress influence (39), and the invasive, parasitic, opportunistic, or pathogenic fungi had close associations with coral disease (e.g., dark spot syndrome and aspergillosis) (88, 89). Thus, corals with high susceptibility to thermal bleaching may have weaker resistance to the increase and invasion of opportunistic or pathogenic fungi in heat-stressed environments. Moreover, there were significant differences in the fungal community structure among distinct coral species in HYI (Fig. 4b); however, there was no significant association between fungal community dissimilarity and coral thermal bleaching susceptibility (Pearson, $R^2 = 0.0014$, $P = 0.735 > .05$; Fig. S1a). Thus, changes in the beta diversity of fungal communities differ from those of bacteria (23, 82, 86, 90). However, fungal alpha diversity has a negative association with fungal beta diversity within the coral holobiont (Pearson, $R^2 = 0.0489$, $P = 0.047 < .05$; Fig. S1b), which was mainly contributed by pathogenic fungi and may have been closely associated with the process of fungal mycoparasitism or hyperparasitism (the functional profile abundance of fungal pathogen was 1.2% in HYI; Fig. 6a) (91).

The fungal indicators of coral thermal bleaching susceptibility and their potentially ecological function

The four fungal indictors Didymellaceae, *Schizophyllum*, *Colletotrichum*, and Chaetomiaceae were identified in corals of HYI in this study and were used to classify the interspecific differences in the fungal community and thermal bleaching susceptibility (Fig. 5e). Although these fungal indicators have rarely been explored or researched in marine ecosystems (91), it is interesting that the vast majority of fungi sampled from marine surfaces or deep-sea environments branch close to or within clades of known terrestrial fungi, suggesting that some core or key ecological function traits may be shared among fungi with adjacent divergence, and many fungi have the ability to easily transition to distinct marine ecosystems (39, 92). The ecological function of fungal indicators in coral holobionts has been speculated by comparing them with fungal communities in distinct creatures or ecosystems. Notably, the fungal indicator Didymellaceae showed high relative abundance in heat-sensitive coral species; this may be closely associated with coral thermal bleaching. Didymellaceae are able to live in the ocean (93) and have also been isolated from sponges (e.g., *Callyspongia* sp.) in coral reefs (94). Many primary plant pathogens have been found in Didymellaceae, such as *Phoma*, *Ascochy*, and *Didymella*, which can lead to serious diseases in Cruciferae and oilseed rape (95, 96). Thus, an increase in the abundance of Didymellaceae may be associated with a reduced stability of coral–Symbiodiniaceae symbioses under thermal stress. Interestingly, *Colletotrichum* was enriched in the fungal community of coral species with intermediate thermal bleaching susceptibility levels (e.g., *F. halicora*), which may be a specific opportunistic plant pathogen that mediates coral bleaching by parasitizing Symbiodiniaceae under heat stress. *Colletotrichum* is recognized as one of the top 10 fungal plant pathogens that can cause anthracnose spots and blights in aerial plants and food crops (97–100). It is worth noting that the *Colletotrichum* has a unique intracellular hemibiotrophic lifestyle, enabling it to establish infection through a brief biotrophic phase, and some species can live in subcuticular tissues (98). This physiological characteristic may provide a basis for the invasion of symbiosomal cells (Symbiodiniaceae microhabitats) into coral gastrodermis (17). Owing to latent infections (101), the destructive and necrotrophic phases of *Colletotrichum* may be activated by heat stress. This induces the necrosis of Symbiodiniaceae cells by producing narrower secondary hyphae, which may lead to coral thermal bleaching (102, 103). This study also found a complex interaction between fungi and Symbiodiniaceae and that the complexity of the SFIN had a significantly negative association with coral thermal tolerance (Fig. 7c).

However, Chaetomiaceae may be beneficial for coral holobionts, which have been identified in aquatic ecosystems and are closely associated with marine invertebrates (e.g., *Cladiella* sp. and *Apostichopus japonicas*) (104–106). Many members of Chaetomiaceae can produce chaetoglobosins, which have strong antibacterial activity (107), and diverse chaetoglobosins have been isolated from *Pocillopora damicornis*-associated Chaetomiaceae (e.g., *Chaetomium globosum* C2F17) in the SCS (106). It has been found that the pathogenic bacteria have the ability to mediate coral thermal bleaching. For example, pathogenic *Vibrio* (*Vibrio shiloi*, *Vibrio coralliilyticus*, and *Vibrio* AK-1), Acidobacteria, and Flavobacteriales are closely associated with coral thermal bleaching (23, 86, 108, 109), and *Escherichia coli* is sustained in the core bacterial microbiota of *P. verrucosa* in thermal tropical coral reefs (85). Thus, heat-sensitive coral species may acclimate to thermal stress by enriching beneficial Chaetomiaceae species with antimicrobial activity against coral pathogens. In addition, it was verified that the fermentation broth extracts of Chaetomiaceae have antioxidant activity and that the antioxidant capacity of the extracts was comparable to that of Vitamin C (110), which may assist coral holobionts in responding to oxidative stress induced by high temperatures. Transcriptomic studies have found that heat stress leads to strong expression of photoprotective coral host pigments (20), and genes involved in cellular and oxidative stress responses of coral hosts are upregulated under heat stress conditions (21, 111–113). Thus, coral species with an intermediate thermal bleaching susceptibility (e.g., *L. phrygia*) may respond

to seawater warming by increasing the abundance of Chaetomiaceae. The fungal indicator *Schizophyllum* might be a beneficial fungus, which is distributed in coral species with intermediate and high susceptibility to thermal bleaching. Furthermore, marine *Schizophyllum* may be derived from terrestrial ecosystems and plays an important role in carbon cycling in the ocean (114). Moreover, it was recently isolated from corals in the tropical coral reefs surrounding Hainan Island (115). Notably, marine *Schizophyllum* has strong anti-*Vibrio* activities, and some nontoxic strains of *Schizophyllum* (e.g., *Schizophyllum commune* MCCCZ16) have efficacy against *vibrio vulnificus* during infection of white shrimp (116). Therefore, *Schizophyllum* may assist heat-sensitive coral holobionts in resisting thermal bleaching mediated by *Vibrio* (23, 109).

Accordingly, Didymellaceae, *Schizophyllum*, *Colletotrichum*, and Chaetomiaceae are potential fungal indicators of coral thermal bleaching susceptibility levels. Pathogenic or opportunistic fungal indicators may be associated with a decrease of the heat tolerance of coral–Symbiodiniaceae symbioses. However, heat-sensitive coral species may enrich potentially beneficial fungi (Chaetomiaceae and *Schizophyllum*) to respond to heat stress and pathogen activity.

The interaction of Symbiodiniaceae and fungi will affect the thermal adaptive potential of coral holobionts

There was a complex interaction between Symbiodiniaceae and fungi in the coral holobionts of HYI (Fig. 7a). Although, the interaction direction between Symbiodiniaceae and fungi in SFIN was not clear, the number of Symbiodiniaceae nodes was significantly higher than that of the fungal nodes in the SFIN (Fig. 7b), implying that the dominant Symbiodiniaceae sub-clade (relative abundance >5%) was the driver in the SFIN. Some dominant members of *Durusdinium* have been found to improve environmental adaptability by inhibiting parasitic symbionts (e.g., *Durusdinium trenchii* and C7) (117, 118). In addition, MENA studies found that dominant Symbiodiniaceae establish many co-occurrence relationships with rare symbiont biospheres and can regulate the Symbiodiniaceae–bacteria interaction network (SBIN) in coral holobionts (37, 38, 85, 117). For instance, *Cladocopium* dominated in the Symbiodiniaceae communities of endemic coral species in tropical and subtropical coral reefs in the SCS (35, 69, 85, 119), which was a driver of SBIN and controlled and regulated microbial networks by cooperating with α- and γ-proteobacteria (85). In addition, coral Symbiodiniaceae communities are assembled by 2–5 to dominant and diverse rare symbionts (64, 120, 121), and dominant Symbiodiniaceae establish the most stable symbioses with coral hosts owing to long-term acclimatization and coevolution (28, 122, 123). These symbioses were found to be optimal for coral growth and development (3), and the dominant Symbiodiniaceae taxa may maintain or improve the health of corals by regulating the SFIN. Topological feature analysis showed that the diameter, centralization, average degree, average path length, and clustering coefficient of the SFIN were characterized by interspecific heterogeneity (Table 2), suggesting that the heat tolerance of the coral holobiont was not affected by the scale, structural robustness, efficiency of information, or energy transport of SFINs (124–127). Moreover, niche specialization of the microbial community of coral holobionts can be reflected by modularity (127, 128), but there was a weak association between the modularity of SFIN and coral heat tolerance in this study. Although heat-sensitive *A. anthocercis* had the highest modularity, which may imply a high degree of niche differentiation of the microbial community constructed by Symbiodiniaceae, fungi might reduce the thermal adaptive potential of coral holobionts, niche specialization of the microbial community, and other topological properties of SFINs, which were mainly shaped by interspecific differences among coral species.

It is worth noting that the complexity and betweenness centrality of the SFIN had negative and positive correlations with coral thermal bleaching tolerance, respectively (Fig. 7c and d). These results indicate that the coexistence pattern and interaction of Symbiodiniaceae and fungi affect the heat tolerance of coral holobionts, and that the decrease in complexity and increase in the betweenness centrality of SFIN may

improve the heat tolerance of coral holobionts. In previous studies, the high complexity of microbial networks indicated stronger stability and stress resistance of microbial communities in terrestrial ecosystems and animal guts (127, 129–131). However, coral holobionts that survive from stressful environments tend to have lower microbial interaction complexity (85, 132). Healthy coral holobionts showed low microbial network complexity under organic pollution, high temperature, low salinity, and acidification conditions, which have been reported in coral reefs in the SCS and western Atlantic at distinct spatial scales (e.g., latitudinal gradient, upwelling zone, and nitrogen content gradient) (85, 133, 134). Interestingly, a large-scale investigation of the coral microbiome showed that an increase in microbial network complexity may reduce the environmental adaptability of coral holobionts, because pathogenic or opportunistic microorganisms are drivers of these increase mechanisms. This indicates the destabilized microbiome and dysbiosis of coral (23, 82). Although these conclusions were suggested by the coral-associated bacterial community, the change in the alpha diversity of fungi was similar to that of bacteria in coral holobionts (28, 44, 86, 87), and the richness index of the fungal community was negatively correlated with coral heat tolerance (Fig. 3b). Therefore, the decrease in network complexity of the SFIN may be attributed to the decline in the parasitism activity of fungi on Symbiodiniaceae. This is closely associated with the regulation and immunity of coral–Symbiodiniaceae symbioses and increases the heat tolerance of coral holobionts (23). In addition, coral-associated microbial interaction networks characterized by high values of betweenness centrality may have stronger resilience because the removal of nodes does not greatly shape the connectivity of others (132, 135). *Pseudodiploria strigose* colonies were able to acclimate to temperature fluctuation in the inner reefs of Bermuda (annual temperature ranged from 13°C to 15°C), and the microbial network betweenness centrality of the surface mucus layer of this species in the inner reef was higher than that in the outer reefs (annual temperature fluctuation was 10°C) (132). Thus, an increase in betweenness centrality potentially confers more resilience to the microbial community composed of Symbiodiniaceae and fungi, which improves the adaptive potential of coral holobionts to heat stress.

Accordingly, the dominant Symbiodiniaceae taxa were drivers of the SFIN, which may affect the health of coral holobionts by regulating the coexistence pattern between Symbiodiniaceae and fungi. The thermal bleaching susceptibility of coral holobionts is closely associated with potential interactions between Symbiodiniaceae and fungi, and the low complexity and high resilience of SFINs may contribute to the stronger heat tolerance of coral holobionts.

Conclusion

This study found that the Symbiodiniaceae community of corals in HYI was dominated by heat-tolerant *Cladocopium* (C3u sub-clade) and *Durusdinium* (D1 and D6 sub-clades), which may provide extra heat-adaptive potential to coral holobionts and assist corals to acclimate to long-term thermal stress. There were no core fungal ASVs in the coral holobiont, suggesting that the fungal community had high interspecific heterogeneity and flexibility. However, fungal diversity and the abundance of pathogens have significantly positive correlations with coral thermal bleaching percentage. Thus, the increase in fungal diversity and pathogen abundance was closely linked to higher thermal bleaching susceptibility in coral holobionts. Notably, there were four distinctive fungal indicators associated with coral species in HYI. These indicators consist of potentially pathogenic Didymellaceae and Chaetomiaceae, as well as speculatively beneficial *Schizophyllum* and *Colletotrichum*, although their function requires further validation. These four fungal indicators exhibit associations with thermal bleaching susceptibility of coral holobionts, varying from high to intermediate levels. Moreover, there were complex interactions between Symbiodiniaceae and fungi in coral holobionts, and the dominant Symbiodiniaceae was the main constructor and driver of SFINs. This may affect the coral heath state by regulating the coexistent pattern of Symbiodiniaceae and fungi. Coral thermal bleaching susceptibility is closely associated with the

topological properties of the SFIN. Low complexity and high betweenness centrality may indicate limitations in fungal parasitism activity and strong microbial network resilience, which will improve the heat tolerance of coral holobionts. Our study highlights the ecological effects of microbiome dynamics and interactions between Symbiodiniaceae and fungi on coral thermal bleaching susceptibility, providing insights into the role of microorganisms and their interaction as drivers of interspecific differences in coral thermal bleaching.

MATERIALS AND METHODS

Coral thermal bleaching percentage and environmental parameter measurements

The information of coral thermal bleaching percentage was obtained and reanalyzed from coral reef survey in the 15–20°N regions (Hainan Island, Xisha Island, and Zhongsha Islands) of SCS in the coral thermal bleaching event of 2020 (136–138). The data set of coral reef surveys of 2020 was constructed by line intercept transect techniques (atoll: 5–15 m; fringing reef: 2–6 m) and Point Intercept Transect video re-sampling (66, 139, 140) according to our benthic surveys and previous studies (137, 140, 141). Coral species were identified following taxonomic criteria (142, 143). The three levels were used to score the degree of thermal bleaching severity: Level 1, minor thermal bleaching and healthy (0%–20% bleached); Level 2, medium thermal bleaching (20%–60% bleached); and Level 3, severe thermal bleaching and dead (60%–100% bleached) (144). The percentage of coral thermal bleaching was determined as the thermal bleaching cover (all three level) of coral species relative to the total cover of this coral species, which can indicate coral thermal bleaching susceptibility (Table 1).

A total of 30 seawater samples (5 L/sample) were collected in six study sites from the outer reef slope and lagoon in HYI. The temperature (°C), salinity (PSU), DO (mg/L), pH, and turbidity (FNU) were measured by ProDSS Multiparameter Digital Water Quality Mater (YSI, USA) at the same time as that of water sample collection. Consequently, the seawater was stored at −80°C for nutrient tests, and NO^{3-} (µmol/L), NO_2^- (µmol/L), NH_4^+ (µmol/L), SiO_3^{2-} (µmol/L), and PO_4^{3-} (µmol/L) were determined using an QuAAtro auto-continuous flow analyzer (SEAL, Germany). In addition, the difference of environmental factors between the outer reef slope and the lagoon in HYI was tested by Welch's *t*-test, and the statistical significance of difference between two groups was examined by the two-tailed Mann–Whitney test using IBM SPSS.v19.

Sample collection and total holobiont DNA extraction

A total of 81 coral samples were collected from seven families, 12 genus, and 18 species with distinct thermal bleaching tolerance in the outer reef slope and lagoon of HYI; these coral species include *G. retiformis*, *A. nana*, *F. halicora*, *A. anthocercis*, *I. palifera*, *I. cuneata*, *G. pectinata*, *A. gemmifera*, *C. aspera*, *Leptoria phrygia*, *P. lutea*, *M. ampliata*, *P. woodjonesi*, *P. versipora*, *D. speciosa*, *P. verrucosa*, *Hydnophora exesa*, and *L. scutaria* (Table 1). At each coral habitat, we collected morphologically distinct colonies along linear transects of at least 10 m apart at depths ranging from 2 to 15 m at each one of the three sites, which were separated by as much as 4 km. Only adult coral colonies have been collected to control for the effect of age on microbial composition (23). Coral fragments (~2–3 cm^2) were obtained by chisel and hammer from a depth range of 2–15 m via SCUBA diving. The coral samples were cleaned by artificial sterile seawater (salinity: 35‰) to ensure they were not disturbed with free-living Symbiodiniaceae and fungi. All fragments were transferred directly in preloaded 2-mL cryotubes containing 95% ethanol or 20% dimethyl sulfoxide buffer (145) and stored at −20°C until DNA extraction. The total holobiont DNA of 18 coral species have been extracted using the DNeasy Plant Mini Kit (Qiagen, Hilden, Germany) and DNeasy Blood and Tissue Kit (Qiagen, Hilden, Germany) and extraction processes according to the manufacturer's instructions.

PCR amplification, next-generation sequencing, and microbiome identification

The Symbiodiniaceae rDNA ITS2 region was amplified with the primer pair ITSintfor2 (5′-GATTGCAGAACTCCGTG-3′) (144) and ITS2-reverse (5′-GGGATCCATATGCTTAAGTTCAG CGGGT-3′) (146). The fungal ITS region was amplified with the primer pair ITS3F (5′-GC ATCGATGAAGAACGCAGC-3′) and ITS4R (5′-TCCTCCGCTTATTGATATGC-3′) (147). PCR was performed with ~10 ng of DNA, 1.6 µL (5 µm) primer, 0.4 µL *Trans* Start Fastplu DNA Polymerase, 0.2 µL BSA, 4 µL 5 × FastPfu Buffer, 2 µL of 2.5 mM dNTPs, and ddH_2O to a total volume of 20 µL. PCR amplification was conducted on an ABI GeneAmp 9700 thermocycle controller with the following program: 3 min at 95°C, followed by 35 cycles of 95°C for 30 s, 55°C for 30 s, 72°C for 45 s, and a final extension at 72°C for 10 min. The PCR products were purified using the QIAquick Gel Extraction Kit (Qiagen, Hilden, Germany), which were pair-end sequenced on an Illumina Miseq platform (Majorbio, Shanghai, China) using 2 × 300 bp mode based on standard protocols after entry quality control and adapter ligation.

Microbiome sequence data processing and ecological indices analysis

Microbiome sequence processing was performed by Quantitative Insights Into Microbial Ecology 2 (QIIME 2) framework (148). Following the removal of primers, the forward and reverse reads were independently truncated to their appropriate lengths, then paired, dereplicated, subjected to quality control, cleaned, and finally clustered into ASV using the denoise-paired method within the DADA2 algorithm (149). For Symbiodiniaceae, the quality-filtered reads were aligned to the ITS2 database using local BLASTN, and the parameters were following the pipeline detailed by Chen et al. (85, 117). To avoid disturbance of multicopy marker and intragenomic variation of the Symbiodiniaceae ITS2 region (150, 151), we used sequence-based ITS2 (sequences were present at a minimum cut-off of >5% for at least 1 of the 81 samples) analysis to identify dominant Symbiodiniaceae sub-clades (69, 85, 117), which were recognized as biologically relevant entities of Symbiodiniaceae (121, 152). The identification of dominant Symbiodiniaceae sub-clades were used to analyze the Symbiodiniaceae community composition. In addition, the ASVs were employed for the analysis of ecological indices, including measures of alpha and beta diversity, within the Symbiodiniaceae community. However, the interpretation of individual base pair differences may introduce ambiguity to the ASVs clustered based on Symbiodiniaceae ITS sequences (153). Therefore, the ASVs of ITS2 were aligned to a non-redundant ITS2 database using local BLASTN, and non-Symbiodiniaceae ASVs were removed (85). The Symbiodiniaceae reads were uniformly rarefied to a consistent sequencing depth of 26,602 reads per sample. For ASVs of fungi, the Naïve–Bayes classifier was trained on the Unite 8.0/ITS fungi database for taxonomic assignment (154), and sequences assigned to chloroplast, mitochondria, eukaryote, and unknown at the phylum level were removed. The fungal reads were rarefied to 26,446 sequences per samples, using 1,000 iterations of random subsampling without replacement. This approach was employed to ensure that the results of fungal community ecological indices (e.g., alpha and beta diversity) can be effectively compared among samples and groups. The alpha (Chao1 richness index) and beta diversity (Bray–Curits dissimilarity) of Symbiodiniaceae and fungi communities among distinct coral species was analyzed by the Vegan package in R (155). The core ASVs of Symbiodiniaceae and fungi were identified by QIIME 2 and Venn diagram visualization (148), and ASVs consistently present in all coral species and >80% of the samples were selected as representative taxa of the core microbiome (17). The IndicSpecies was employed to identify the indicators of coral-associated Symbiodiniaceae (dominant sub-clades) and fungi (fungal ASV) using the following parameters: minimum specificity and minimum sensitivity set to 70%, P value < 0.05 and 1,000 permutations (156, 157). The relative abundance of indicators of Symbiodiniaceae and fungi was drawn as heat map. The phylogenetic tree was constructed by sequences of indicators of dominant Symbiodiniaceae sub-clades and potential ancestor of *Cladocopium* (C1 and C3 sub-clades) using

maximum likelihood methods (60), which was aimed to speculate on the potential thermal tolerance of Symbiodiniaceae (31, 35, 69). The robustness of the tree was assessed with 1,000 bootstrap replicates. The FUNGuild tool was used to perform the prediction of fungal ecological function groups (158), and the percentages of fungal functional groups were falling into the categories of "unknown" and "known," in addition to those known functional groups with relative abundance exceeding 1% of the known functional groups which were visualized by the ggplot2 package in R.

Molecular ecological network constructed and topological property analysis

To explore the potential and complexed interactions between Symbiodiniaceae and fungi in coral holobiont, the SFIN was inferred by CoNet plugin in Cytoscape 3.9.1 (159, 160). Briefly, the dominant Symbiodiniaceae sub-clades and fungal ASVs were used to construct the data set, and the screening threshold has been set as taxa present in at least two samples and has more than 50 reads. The pairwise correlations among microbial taxa in different coral species were estimated by two measures of correlations (Pearson and Spearman correlations), one measure of similarities (mutual information), and two measures of dissimilarity (Bary–Curtis and Kullback–Leibler dissimilarity). Primarily, 1,000 positive and 1,000 negative edges were retrieved as thresholds for five measures, and 1,000 normalized permutations and 1,000 bootstrap scores were generated to mitigate the combinatorial bias. Brown's method was used to calculate and merge the measure-specific *P* value (161), and the multiple comparisons was corrected by the Benjamini–Hochberg procedure (162). Moreover, only statistically significant correlations (*P* values < 0.05) were accepted for SFIN analysis. Subsequently, the visualization of SFIN was conducted with Gephi 0.9.7 and Cytoscape 3.9.1, and only co-occurrence correlations were drawn in figure.

The topological properties of SFIN were calculated using the igraph package in R, which include the average degree, network diameter, network centralization, average path length, clustering coefficient, modularity, and betweenness centrality. In general, the network diameter is defined as the indicator of the network scale (127). The average degree describes the average number of interactions per node, which can indicate the intensity of interaction among microbial taxa (125, 126). The shortest network distance between all pairs of microbial taxa was measured by average path length, which has close association with the efficiency of energy or information transmission within the network (124, 134, 163). The clustering coefficient was known as a measure of degree to which nodes in a network tend to cluster together, which suggest stability and robustness of the microbial interaction network structure (126, 127). The modularity of microbial networks was able to reflect the degree to which a network is divided into individual compartments, and nodes have strong connections with other nodes within the same module and have weak association with nodes in other modules (127, 164). Thus, the modularity was used to estimate the niche differentiation and specialization of microbial community. In addition, betweenness centrality calculates the shortest path through a microbial network and keeps record of how many times a node in a network is traversed (165), which can reflect the resilience and connectivity of microbial community (132, 135). The complexity of SFIN was determined as linkage density (links per node) among distinct coral species (130). To identify the key driver of SFIN, the percentage of the network node for Symbiodiniaceae and fungi was calculated.

Statistical analyses

The interspecific differences of the Chao1 richness index of Symbiodiniaceae and fungal community were assessed by the Kruskal–Wallis test by performing in GraphPad Prism 8, and the Dunn test was used for *post hoc* multiple comparisons of significant Kruskal–Wallis test results. PERMANOVA was used to test the significance of interspecific differences of Symbiodiniaceae and fungal community structure with 9,999 permutation-based Bray–Curtis dissimilarity matrix. The results of PERMANOVA were visualized by the PCoA generated by the Bray–Curtis distance in the Vegan package in R (155).

The SLR was used to construct the correlations between ecological indices (e.g., Chao1 richness index, abundance of pathogenic fungi, and topological parameter of SFIN) and coral thermal bleaching percentage. Pearson's correlation was employed to calculate the coefficient of determination (R^2) using GraphPad Prism 8, and the statistical significance was considered at $P < 0.05$. In addition, the difference of the percentage of network node between Symbiodiniaceae and fungi in SFIN was tested by Welch *t*-test, and the two-tailed Mann–Whitney test was conducted to examine the statistical significance of the difference between two groups using IBM SPSS.v19.

ACKNOWLEDGMENTS

We thank Ms. Zhixian Li for improving the quality of the English writing.

This study was supported by the National Natural Science Foundation of China (no. 42090041, 42306165, and 42030502), the Self-Topic Project of Guangxi Laboratory on the Study of Coral Reefs in the South China Sea (no. GXLSCRSCS2021103), and the Central Public-Interest Scientific Institution Basal Research Fund (PM-zx703-202105-176, PM-zx703-202004-143).

AUTHOR AFFILIATIONS

[1]Guangxi Laboratory on the Study of Coral Reefs in the South China Sea, Coral Reef Research Center of China, School of Marine Sciences, Guangxi University, Nanning, China
[2]Southern Marine Science and Engineering Guangdong Laboratory (Guangzhou), Guangzhou, China
[3]Key Laboratory of Environmental Change and Resource Use in Beibu Gulf, Ministry of Education, Nanning Normal University, Nanning, China
[4]South China Institute of Environmental Sciences, MEE, Guangzhou, China

AUTHOR ORCIDs

Biao Chen http://orcid.org/0000-0001-9622-6423
Kefu Yu http://orcid.org/0000-0003-3409-9945

FUNDING

Funder	Grant(s)	Author(s)
MOST | National Natural Science Foundation of China (NSFC)	42090041, 42030502	Kefu Yu
MOST | National Natural Science Foundation of China (NSFC)	42306165	Biao Chen
Self-Topic Project of Guangxi Laboratory on the Study of Coral Reefs in the South China Sea	GXLSCRSCS2021103	Biao Chen
Central Public-Interest Scientific Institution Basal Fund	PM-zx703-202105-176, PM-zx703-202004-143	Lijia Xu

AUTHOR CONTRIBUTIONS

Biao Chen, Conceptualization, Data curation, Formal analysis, Funding acquisition, Investigation, Methodology, Resources, Software, Supervision, Validation, Visualization, Writing – original draft, Writing – review and editing | Yuxin Wei, Data curation, Formal analysis, Investigation, Methodology, Resources, Visualization, Writing – review and editing | Kefu Yu, Conceptualization, Data curation, Formal analysis, Funding acquisition, Methodology, Project administration, Resources, Supervision, Validation, Writing – original draft, Writing – review and editing | Yanting Liang, Data curation, Methodology, Resources, Software, Validation, Writing – review and editing | Xiaopeng Yu, Data curation, Investigation, Methodology, Resources, Writing – review and editing | Zhiheng Liao, Data curation, Investigation, Validation, Visualization, Writing – review and editing

| Zhenjun Qin, Investigation, Methodology, Software, Writing – review and editing | Lijia Xu, Funding acquisition, Investigation, Resources, Writing – review and editing | Zeming Bao, Investigation, Software, Writing – review and editing

DATA AVAILABILITY

The NGS raw read data set of Symbiodiniaceae ITS2 and Fungal ITS amplicons has been stored in the NCBI Sequence Read Archive database (SRA), with the accession numbers SRP432680 and SRP432640 under BioProject numbers PRJNA955669 and PRJNA955684, respectively.

ADDITIONAL FILES

The following material is available online.

Supplemental Material

Table S1 and Table S2; Figure S1 (AEM01939-23-s0001.pdf). Environmental factors, indicative capacity values of fungi and the correlation among fungal community dissimilarity, coral thermal bleaching susceptibility and Chao1 richness index of fungi.

REFERENCES

1. Blackall LL, Wilson B, van Oppen MJH. 2015. Coral-the world's most diverse symbiotic ecosystem. Mol Ecol 24:5330–5347. https://doi.org/10.1111/mec.13400
2. Fisher R, O'Leary RA, Low-Choy S, Mengersen K, Knowlton N, Brainard RE, Caley MJ. 2015. Species richness on coral reefs and the pursuit of convergent global estimates. Curr Biol 25:500–505. https://doi.org/10.1016/j.cub.2014.12.022
3. Voolstra CR, Suggett DJ, Peixoto RS, Parkinson JE, Quigley KM, Silveira CB, Sweet M, Muller EM, Barshis DJ, Bourne DG, Aranda M. 2021. Extending the natural adaptive capacity of coral holobionts. Nat Rev Earth Environ 2:747–762. https://doi.org/10.1038/s43017-021-00214-3
4. Hughes TP, Kerry JT, Álvarez-Noriega M, Álvarez-Romero JG, Anderson KD, Baird AH, Babcock RC, Beger M, Bellwood DR, Berkelmans R, et al. 2017. Global warming and recurrent mass bleaching of corals. Nature 543:373–377. https://doi.org/10.1038/nature21707
5. Perry CT, Morgan KM. 2017. Bleaching drives collapse in reef carbonate budgets and reef growth potential on southern Maldives reefs. Sci Rep 7:40581. https://doi.org/10.1038/srep40581
6. Claar DC, Starko S, Tietjen KL, Epstein HE, Cunning R, Cobb KM, Baker AC, Gates RD, Baum JK. 2020. Dynamic symbioses reveal pathways to coral survival through prolonged heatwaves. Nat Commun 11:6097. https://doi.org/10.1038/s41467-020-19169-y
7. Silverstein RN, Cunning R, Baker AC. 2015. Change in algal symbiont communities after bleaching, not prior heat exposure, increases heat tolerance of reef corals. Glob Chang Biol 21:236–249. https://doi.org/10.1111/gcb.12706
8. Stuart-Smith RD, Brown CJ, Ceccarelli DM, Edgar GJ. 2018. Ecosystem restructuring along the Great Barrier Reef following mass coral bleaching. Nature 560:92–96. https://doi.org/10.1038/s41586-018-0359-9
9. Hughes TP, Kerry JT, Baird AH, Connolly SR, Dietzel A, Eakin CM, Heron SF, Hoey AS, Hoogenboom MO, Liu G, McWilliam MJ, Pears RJ, Pratchett MS, Skirving WJ, Stella JS, Torda G. 2018. Global warming transforms coral reef assemblages. Nature 556:492–496. https://doi.org/10.1038/s41586-018-0041-2
10. Hughes TP, Kerry JT, Simpson T. 2018. Large - scale bleaching of corals on the Great Barrier Reef. Ecology 99:501. https://doi.org/10.1002/ecy.2092
11. Baum JK, Claar DC, Tietjen KL, Magel JMT, Maucieri DG, Cobb KM, McDevitt-Irwin JM. 2023. Transformation of coral communities subjected to an unprecedented heatwave is modulated by local disturbance. Sci Adv 9:eabq5615. https://doi.org/10.1126/sciadv.abq5615
12. Frölicher TL, Fischer EM, Gruber N. 2018. Marine heatwaves under global warming. Nature 560:360–364. https://doi.org/10.1038/s41586-018-0383-9
13. Oliver ECJ, Burrows MT, Donat MG, Sen Gupta A, Alexander LV, Perkins-Kirkpatrick SE, Benthuysen JA, Hobday AJ, Holbrook NJ, Moore PJ, Thomsen MS, Wernberg T, Smale DA. 2019. Projected marine heatwaves in the 21st century and the potential for ecological impact. Front Mar Sci 6:734. https://doi.org/10.3389/fmars.2019.00734
14. van Hooidonk R, Maynard J, Tamelander J, Gove J, Ahmadia G, Raymundo L, Williams G, Heron SF, Planes S. 2016. Local-scale projections of coral reef futures and implications of the Paris Agreement. Sci Rep 6:39666. https://doi.org/10.1038/srep39666
15. Smith EG, Hazzouri KM, Choi JY, Delaney P, Al-Kharafi M, Howells EJ, Aranda M, Burt JA. 2022. Signatures of selection underpinning rapid coral adaptation to the world's warmest reefs. Sci Adv 8:eabl7287. https://doi.org/10.1126/sciadv.abl7287
16. Rosenberg E, Koren O, Reshef L, Efrony R, Zilber-Rosenberg I. 2007. The role of microorganisms in coral health, disease and evolution. Nat Rev Microbiol 5:355–362. https://doi.org/10.1038/nrmicro1635
17. Hernandez-Agreda A, Gates RD, Ainsworth TD. 2017. Defining the core microbiome in corals' microbial soup. Trends Microbiol 25:125–140. https://doi.org/10.1016/j.tim.2016.11.003
18. Bay RA, Palumbi SR. 2014. Multilocus adaptation associated with heat resistance in reef-building corals. Curr Biol 24:2952–2956. https://doi.org/10.1016/j.cub.2014.10.044
19. Thomas L, Rose NH, Bay RA, López EH, Morikawa MK, Ruiz-Jones L, Palumbi SR. 2018. Mechanisms of thermal tolerance in reef-building corals across a fine-grained environmental mosaic: lessons from Ofu, American Samoa. Front Mar Sci 4:434. https://doi.org/10.3389/fmars.2017.00434
20. Bollati E, D'Angelo C, Alderdice R, Pratchett M, Ziegler M, Wiedenmann J. 2020. Optical feedback loop involving dinoflagellate symbiont and scleractinian host drives colorful coral bleaching. Curr Biol 30:2433–2445. https://doi.org/10.1016/j.cub.2020.04.055
21. Yu X, Yu K, Liao Z, Liang J, Deng C, Huang W, Huang Y. 2020. Potential molecular traits underlying environmental tolerance of *Pavona decussata* and *Acropora pruinosa* in Weizhou Island, northern South China Sea. Mar Pollut Bull 156:111199. https://doi.org/10.1016/j.marpolbul.2020.111199
22. Thurber RV, Payet JP, Thurber AR, Correa AMS. 2017. Virus–host interactions and their roles in coral reef health and disease. Nat Rev Microbiol 15:205–216. https://doi.org/10.1038/nrmicro.2016.176

23. van Oppen MJH, Blackall LL. 2019. Coral microbiome dynamics, functions and design in a changing world. Nat Rev Microbiol 17:557–567. https://doi.org/10.1038/s41579-019-0223-4
24. Grottoli AG, Warner ME, Levas SJ, Aschaffenburg MD, Schoepf V, McGinley M, Baumann J, Matsui Y. 2014. The cumulative impact of annual coral bleaching can turn some coral species winners into losers. Glob Chang Biol 20:3823–3833. https://doi.org/10.1111/gcb.12658
25. Ziegler M, Seneca FO, Yum LK, Palumbi SR, Voolstra CR. 2017. Bacterial community dynamics are linked to patterns of coral heat tolerance. Nat Commun 8:14213. https://doi.org/10.1038/ncomms14213
26. Qin Z, Yu K, Chen B, Wang Y, Liang J, Luo W, Xu L, Huang X. 2019. Diversity of Symbiodiniaceae in 15 coral species from the Southern South China Sea: potential relationship with coral thermal adaptability. Front Microbiol 10:2343. https://doi.org/10.3389/fmicb.2019.02343
27. Qin Z, Yu K, Liang J, Yao Q, Chen B. 2020. Significant changes in microbial communities associated with reef corals in the southern South China Sea during the 2015/2016 global - scale coral bleaching event. J Geophys Res Oceans 125. https://doi.org/10.1029/-2019JC015579
28. Chavanich S, Kusdianto H, Kullapanich C, Jandang S, Wongsawaeng D, Ouazzani J, Viyakarn V, Somboonna N. 2022. Microbiomes of healthy and bleached corals during a 2016 thermal bleaching event in the Andaman Sea of Thailand. Front Mar Sci 9:763421. https://doi.org/10.3389/fmars.2022.763421
29. LaJeunesse TC, Parkinson JE, Gabrielson PW, Jeong HJ, Reimer JD, Voolstra CR, Santos SR. 2018. Systematic revision of Symbiodiniaceae highlights the antiquity and diversity of coral endosymbionts. Curr Biol 28:2570–2580. https://doi.org/10.1016/j.cub.2018.07.008
30. Baker AC, Starger CJ, McClanahan TR, Glynn PW. 2004. Corals' adaptive response to climate change. Nature 430:741. https://doi.org/10.1038/430741a
31. LaJeunesse TC, Pettay DT, Sampayo EM, Phongsuwan N, Brown B, Obura DO, Hoegh - Guldberg O, Fitt WK. 2010. Long - standing environmental conditions, geographic isolation and host–symbiont specificity influence the relative ecological dominance and genetic diversification of coral endosymbionts in the genus *Symbiodinium*. J Biogeogr37:785–800. https://doi.org/10.1111/j.1365-2699.2010.02273.x
32. Reimer JD, Takishita K, Maruyama T. 2006. Molecular identification of symbiotic dinoflagellates (*Symbiodinium* spp.) from *Palythoa* spp. (Anthozoa: Hexacorallia) in Japan. Coral Reefs 25:521–527. https://doi.org/10.1007/s00338-006-0151-4
33. Grupstra CGB, Coma R, Ribes M, Leydet KP, Parkinson JE, McDonald K, Catllà M, Voolstra CR, Hellberg ME, Coffroth MA. 2017. Evidence for coral range expansion accompanied by reduced diversity of *Symbiodinium* genotypes. Coral Reefs 36:981–985. https://doi.org/10.1007/s00338-017-1589-2
34. Brener-Raffalli K, Clerissi C, Vidal-Dupiol J, Adjeroud M, Bonhomme F, Pratlong M, Aurelle D, Mitta G, Toulza E. 2018. Thermal regime and host clade, rather than geography, drive *Symbiodinium* and bacterial assemblages in the scleractinian coral *Pocillopora damicornis sensu lato*. Microbiome 6:39. https://doi.org/10.1186/s40168-018-0423-6
35. Chen B, Yu K, Liang J, Huang W, Wang G, Su H, Qin Z, Huang X, Pan Z, Luo W, Luo Y, Wang Y. 2019. Latitudinal variation in the molecular diversity and community composition of Symbiodiniaceae in coral from the South China Sea. Front Microbiol 10:1278. https://doi.org/10.3389/fmicb.2019.01278
36. Osman EO, Suggett DJ, Voolstra CR, Pettay DT, Clark DR, Pogoreutz C, Sampayo EM, Warner ME, Smith DJ. 2020. Coral microbiome composition along the northern Red Sea suggests high plasticity of bacterial and specificity of endosymbiotic dinoflagellate communities. Microbiome 8:8. https://doi.org/10.1186/s40168-019-0776-5
37. Ziegler M, Eguíluz VM, Duarte CM, Voolstra CR. 2018. Rare symbionts may contribute to the resilience of coral–algal assemblages. ISME J 12:161–172. https://doi.org/10.1038/ismej.2017.151
38. Chen B, Yu K, Qin Z, Liang J, Wang G, Huang X, Wu Q, Jiang L. 2020. Dispersal, genetic variation, and symbiont interaction network of heat-tolerant endosymbiont *Durusdinium trenchii*: insights into the adaptive potential of coral to climate change. Sci Total Environ 723:138026. https://doi.org/10.1016/j.scitotenv.2020.138026
39. Roik A, Reverter M, Pogoreutz C. 2022. A roadmap to understanding diversity and function of coral reef-associated fungi. FEMS Microbiol Rev 46:fuac028. https://doi.org/10.1093/femsre/fuac028
40. Golubic S, Radtke G, Le Campion-Alsumard T. 2005. Endolithic fungi in marine ecosystems. Trends Microbiol 13:229–235. https://doi.org/10.1016/j.tim.2005.03.007
41. Amend A, Burgaud G, Cunliffe M, Edgcomb VP, Ettinger CL, Gutiérrez MH, Heitman J, Hom EFY, Ianiri G, Jones AC, Kagami M, Picard KT, Quandt CA, Raghukumar S, Riquelme M, Stajich J, Vargas-Muñiz J, Walker AK, Yarden O, Gladfelter AS. 2019. Fungi in the marine environment: open questions and unsolved problems. mBio 10:e01189-18. https://doi.org/10.1128/mBio.01189-18
42. Rabbani G, Huang D, Wainwright BJ. 2021. The mycobiome of *Pocillopora acuta* in Singapore. Coral Reefs 40:1419–1427. https://doi.org/10.1007/s00338-021-02152-4
43. Cárdenas A, Raina J-B, Pogoreutz C, Rädecker N, Bougoure J, Guagliardo P, Pernice M, Voolstra CR. 2022. Greater functional diversity and redundancy of coral endolithic microbiomes align with lower coral bleaching susceptibility. ISME J 16:2406–2420. https://doi.org/10.1038/s41396-022-01283-y
44. Amend AS, Barshis DJ, Oliver TA. 2012. Coral-associated marine fungi form novel lineages and heterogeneous assemblages. ISME J 6:1291–1301. https://doi.org/10.1038/ismej.2011.193
45. Lifshitz N, Hazanov L, Fine M, Yarden O. 2020. Seasonal variations in the culturable mycobiome of *Acropora loripes* along a depth gradient. Microorganisms 8:1139. https://doi.org/10.3390/microorganisms8081139
46. Geiser DM, Taylor JW, Ritchie KB, Smith GW. 1998. Cause of sea fan death in the West Indies. Nature 394:137–138. https://doi.org/10.1038/28079
47. Ainsworth TD, Fordyce AJ, Camp EF. 2017. The other microeukaryotes of the coral reef microbiome. Trends Microbiol 25:980–991. https://doi.org/10.1016/j.tim.2017.06.007
48. Gladfelter AS, James TY, Amend AS. 2019. Marine fungi. Curr Biol 29:R191–R195. https://doi.org/10.1016/j.cub.2019.02.009
49. Sully S, Burkepile DE, Donovan MK, Hodgson G, van Woesik R. 2019. A global analysis of coral bleaching over the past two decades. Nat Commun 10:1264. https://doi.org/10.1038/s41467-019-09238-2
50. Qin Z, Yu K, Wang Y, Xu L, Huang X, Chen B, Li Y, Wang W, Pan Z. 2019. Spatial and intergeneric variation in physiological indicators of corals in the South China Sea: insights into their current state and their adaptability to environmental stress. J Geophys Res Oceans 124:3317–3332. https://doi.org/10.1029/2018JC014648
51. Liang Y, Yu K, Pan Z, Qin Z, Liao Z, Chen B, Huang X, Xu L. 2021. Intergeneric and geomorphological variations in Symbiodiniaceae densities of reef-building corals in an isolated atoll, central South China Sea. Mar Pollut Bull 163:111946. https://doi.org/10.1016/j.marpolbul.2020.111946
52. Liao Z, Yu K, Chen B, Huang X, Qin Z, Yu X, Blakeslee A. 2021. Spatial distribution of benthic algae in the South China Sea: responses to gradually changing environmental factors and ecological impacts on coral communities. Divers Distrib27:929–943. https://doi.org/10.1111/ddi.13243
53. Pan Z. 2017. Interspecies and spatial diversity of *Symbiodinium* density in coral species from the Huangyan Island,and its ecological significance. Guangxi University
54. Thomas L, Kendrick GA, Kennington WJ, Richards ZT, Stat M. 2014. Exploring *Symbiodinium* diversity and host specificity in *Acropora* corals from geographical extremes of Western Australia with 454 amplicon pyrosequencing. Mol Ecol 23:3113–3126. https://doi.org/10.1111/mec.12801
55. Tong H, Cai L, Zhou G, Yuan T, Zhang W, Tian R, Huang H, Qian PY. 2017. Temperature shapes coral-algal symbiosis in the South China Sea. Sci Rep 7:40118. https://doi.org/10.1038/srep40118
56. Pettay DT, Wham DC, Smith RT, Iglesias-Prieto R, LaJeunesse TC. 2015. Microbial invasion of the Caribbean by an Indo-Pacific coral zooxanthella. Proc Natl Acad Sci U S A 112:7513–7518. https://doi.org/10.1073/pnas.1502283112
57. Yu K. 2000. The recent fifty years high-resolution climate of Nansha Islands recorded in reef coral. Guangzhou Guangzhou Institute of Geochemistry, Chinese Academy of Sciences

58. Zuo X, Su F, Wu W, Chen Z, Shi W. 2015. Spatial and temporal variability of thermal stress to China's coral reefs in South China Sea. Chin Geogr Sci 25:159–173. https://doi.org/10.1007/s11769-015-0741-6
59. Qin Z, Chen S, Yu K, Chen B, Pan N, Wei X. 2022. Lagoon coral microbiomes and their potential relationship with adaptation of coral holobionts to extreme high-temperature environments. Mar Ecol Prog Ser 699:19–32. https://doi.org/10.3354/meps14173
60. Lajeunesse TC. 2005. "Species" radiations of symbiotic dinoflagellates in the Atlantic and Indo-Pacific since the Miocene-Pliocene transition. Mol Biol Evol 22:570–581. https://doi.org/10.1093/molbev/msi042
61. Lee LK, Leaw CP, Lee LC, Lim ZF, Hii KS, Chan AA, Gu H, Lim PT. 2022. Molecular diversity and assemblages of coral symbionts (Symbiodiniaceae) in diverse scleractinian coral species. Mar Environ Res 179:105706. https://doi.org/10.1016/j.marenvres.2022.105706
62. Chankong A, Kongjandtre N, Senanan W, Manthachitra V. 2020. Community composition of Symbiodiniaceae among four scleractinian corals in the eastern Gulf of Thailand. Reg Stud Mar Sci33:100918. https://doi.org/10.1016/j.rsma.2019.100918
63. Torres AF, Valino DAM, Ravago-Gotanco R. 2021. Zooxanthellae diversity and coral-symbiont associations in the Philippine Archipelago: specificity and adaptability across thermal gradients. Front Mar Sci 8:731023. https://doi.org/10.3389/fmars.2021.731023
64. Boulotte NM, Dalton SJ, Carroll AG, Harrison PL, Putnam HM, Peplow LM, van Oppen MJ. 2016. Exploring the *Symbiodinium* rare biosphere provides evidence for symbiont switching in reef-building corals. ISME J 10:2693–2701. https://doi.org/10.1038/ismej.2016.54
65. LaJeunesse TC, Forsman ZH, Wham DC. 2016. An Indo-West Pacific 'zooxanthella'invasive to the western Atlantic finds its way to the Eastern Pacific via an introduced Caribbean coral. Coral Reefs 35:577–582. https://doi.org/10.1007/s00338-015-1388-6
66. Liao Z. 2021. Spatial distribution of coral community and benthic algae and their ecological impacts across the South China Sea. Guangxi University
67. Pochon X, LaJeunesse TC, Pawlowski J. 2004. Biogeographic partitioning and host specialization among foraminiferan dinoflagellate symbionts (Symbiodinium; Dinophyta). Mar Biol146:17–27. https://doi.org/10.1007/s00227-004-1427-2
68. Ziegler M, Roder C, Büchel C, Voolstra CR. 2015. Niche acclimatization in Red Sea corals is dependent on flexibility of host-symbiont association. Mar Ecol Prog Ser 533:149–161. https://doi.org/10.3354/meps11365
69. Qin Z, Yu K, Chen S, Chen B, Liang J, Yao Q, Yu X, Liao Z, Deng C, Liang Y. 2021. Microbiome of juvenile corals in the outer reef slope and lagoon of the South China Sea: insight into coral acclimatization to extreme thermal environments. Environ Microbiol 23:4389–4404. https://doi.org/10.1111/1462-2920.15624
70. Yarden O, Ainsworth TD, Roff G, Leggat W, Fine M, Hoegh-Guldberg O. 2007. Increased prevalence of ubiquitous ascomycetes in an acropoid coral (*Acropora formosa*) exhibiting symptoms of brown band syndrome and skeletal eroding band disease. Appl Environ Microbiol 73:2755–2757. https://doi.org/10.1128/AEM.02738-06
71. Thurber RV, Willner‐Hall D, Rodriguez‐Mueller B, Desnues C, Edwards RA, Angly F, Dinsdale E, Kelly L, Rohwer F. 2009. Metagenomic analysis of stressed coral holobionts. Environ Microbiol11:2148–2163. https://doi.org/10.1111/j.1462-2920.2009.01935.x
72. Wegley L, Edwards R, Rodriguez-Brito B, Liu H, Rohwer F. 2007. Metagenomic analysis of the microbial community associated with the coral *Porites astreoides*. Environ Microbiol 9:2707–2719. https://doi.org/10.1111/j.1462-2920.2007.01383.x
73. Góes-Neto A, Marcelino VR, Verbruggen H, da Silva FF, Badotti F. 2020. Biodiversity of endolithic fungi in coral skeletons and other reef substrates revealed with 18S rDNA metabarcoding. Coral Reefs 39:229–238. https://doi.org/10.1007/s00338-019-01880-y
74. Paulino GVB, Félix CR, Landell MF. 2020. Diversity of filamentous fungi associated with coral and sponges in coastal reefs of northeast Brazil. J Basic Microbiol 60:103–111. https://doi.org/10.1002/jobm.201900394
75. Kusdianto H, Kullapanich C, Palasuk M, Jandang S, Pattaragulwanit K, Ouazzani J, Chavanich S, Viyakarn V, Somboonna N. 2021. Microbiomes of healthy and bleached corals during a 2016 thermal bleaching event in the upper Gulf of Thailand. Front Mar Sci 8:643962. https://doi.org/10.3389/fmars.2021.643962
76. Bonthond G, Merselis DG, Dougan KE, Graff T, Todd W, Fourqurean JW, Rodriguez-Lanetty M. 2018. Inter-domain microbial diversity within the coral holobiont *Siderastrea siderea* from two depth habitats. PeerJ 6:e4323. https://doi.org/10.7717/peerj.4323
77. D Ainsworth T, Krause L, Bridge T, Torda G, Raina J-B, Zakrzewski M, Gates RD, Padilla-Gamiño JL, Spalding HL, Smith C, Woolsey ES, Bourne DG, Bongaerts P, Hoegh-Guldberg O, Leggat W. 2015. The coral core microbiome identifies rare bacterial taxa as ubiquitous endosymbionts. ISME J 9:2261–2274. https://doi.org/10.1038/ismej.2015.39
78. Hernandez-Agreda A, Leggat W, Bongaerts P, Ainsworth TD, Rosenberg E, Azam F. 2016. The microbial signature provides insight into the mechanistic basis of coral success across reef habitats. mBio 7:e00560-16. https://doi.org/10.1128/mBio.00560-16
79. Yu X, Yu K, Chen B, Liao Z, Liang J, Yao Q, Qin Z, Wang H, Yu J. 2021. Different responses of scleractinian coral *Acropora pruinosa* from Weizhou Island during extreme high temperature events. Coral Reefs 40:1697–1711. https://doi.org/10.1007/s00338-021-02182-y
80. Meron D, Atias E, Iasur Kruh L, Elifantz H, Minz D, Fine M, Banin E. 2011. The impact of reduced pH on the microbial community of the coral *Acropora eurystoma*. ISME J 5:51–60. https://doi.org/10.1038/ismej.2010.102
81. Jessen C, Villa Lizcano JF, Bayer T, Roder C, Aranda M, Wild C, Voolstra CR, Gilbert JA. 2013. In-situ effects of eutrophication and overfishing on physiology and bacterial diversity of the Red Sea coral *Acropora hemprichii*. PLoS One 8:e62091. https://doi.org/10.1371/journal.pone.0062091
82. Zaneveld JR, Burkepile DE, Shantz AA, Pritchard CE, McMinds R, Payet JP, Welsh R, Correa AMS, Lemoine NP, Rosales S, Fuchs C, Maynard JA, Thurber RV. 2016. Overfishing and nutrient pollution interact with temperature to disrupt coral reefs down to microbial scales. Nat Commun 7:11833. https://doi.org/10.1038/ncomms11833
83. Ziegler M, Roik A, Porter A, Zubier K, Mudarris MS, Ormond R, Voolstra CR. 2016. Coral microbial community dynamics in response to anthropogenic impacts near a major city in the central Red Sea. Mar Pollut Bull 105:629–640. https://doi.org/10.1016/j.marpolbul.2015.12.045
84. Ziegler M, Grupstra CGB, Barreto MM, Eaton M, BaOmar J, Zubier K, Al-Sofyani A, Turki AJ, Ormond R, Voolstra CR. 2019. Coral bacterial community structure responds to environmental change in a host-specific manner. Nat Commun 10:3092. https://doi.org/10.1038/s41467-019-10969-5
85. Chen B, Yu K, Liao Z, Yu X, Qin Z, Liang J, Wang G, Wu Q, Jiang L. 2021. Microbiome community and complexity indicate environmental gradient acclimatisation and potential microbial interaction of endemic coral holobionts in the South China Sea. Sci Total Environ 765:142690. https://doi.org/10.1016/j.scitotenv.2020.142690
86. McDevitt-Irwin JM, Baum JK, Garren M, Vega Thurber RL. 2017. Responses of coral-associated bacterial communities to local and global stressors. Front Mar Sci 4:262. https://doi.org/10.3389/fmars.2017.00262
87. Welsh RM, Zaneveld JR, Rosales SM, Payet JP, Burkepile DE, Thurber RV. 2016. Bacterial predation in a marine host-associated microbiome. ISME J 10:1540–1544. https://doi.org/10.1038/ismej.2015.219
88. Alker AP, Smith GW, Kim K. 2001. Characterization of Aspergillus sydowii (Thom et Church), a fungal pathogen of Caribbean sea fan corals. Hydrobiologia 460:105–111. https://doi.org/10.1023/A:1013145524136
89. Sweet M, Burn D, Croquer A, Leary P, Bereswill S. 2013. Characterisation of the bacterial and fungal communities associated with different lesion sizes of dark spot syndrome occurring in the coral *Stephanocoenia intersepta*. PLoS One 8:e62580. https://doi.org/10.1371/journal.pone.0062580
90. Morrow KM, Moss AG, Chadwick NE, Liles MR. 2012. Bacterial associates of two Caribbean coral species reveal species-specific distribution and geographic variability. Appl Environ Microbiol 78:6438–6449. https://doi.org/10.1128/AEM.01162-12
91. Grossart H-P, Van den Wyngaert S, Kagami M, Wurzbacher C, Cunliffe M, Rojas-Jimenez K. 2019. Fungi in aquatic ecosystems. Nat Rev Microbiol 17:339–354. https://doi.org/10.1038/s41579-019-0175-8

92. Simonato F, Campanaro S, Lauro FM, Vezzi A, D'Angelo M, Vitulo N, Valle G, Bartlett DH. 2006. Piezophilic adaptation: a genomic point of view. J Biotechnol 126:11–25. https://doi.org/10.1016/j.jbiotec.2006.03.038
93. Suetrong S, Schoch CL, Spatafora JW, Kohlmeyer J, Volkmann-Kohlmeyer B, Sakayaroj J, Phongpaichit S, Tanaka K, Hirayama K, Jones EBG. 2009. Molecular systematics of the marine *Dothideomycetes*. Stud Mycol 64:155–173S6. https://doi.org/10.3114/sim.2009.64.09
94. Tian Y, Lin X, Zhou X, Liu Y. 2018. Phenol derivatives from the sponge-derived fungus *Didymellaceae* sp. SCSIO F46. Front Chem 6:536. https://doi.org/10.3389/fchem.2018.00536
95. Gugel RK, Petrie GA. 1992. History, occurrence, impact, and control of blackleg of rapeseed. Can J Plant Pathol 14:36–45. https://doi.org/10.1080/07060669209500904
96. Fitt BDL, Brun H, Barbetti MJ, Rimmer SR. 2006. World-wide importance of phoma stem canker (*Leptosphaeria maculans* and *L. biglobosa*) on oilseed rape (*Brassica napus*). Eur J Plant Pathol 114:3–15. https://doi.org/10.1007/s10658-005-2233-5
97. Cannon PF, Damm U, Johnston PR, Weir BS. 2012. Colletotrichum: current status and future directions. Stud Mycol 73:181–213. https://doi.org/10.3114/sim0014
98. Dean R, Van Kan JAL, Pretorius ZA, Hammond-Kosack KE, Di Pietro A, Spanu PD, Rudd JJ, Dickman M, Kahmann R, Ellis J, Foster GD. 2012. The top 10 fungal pathogens in molecular plant pathology. Mol Plant Pathol 13:414–430. https://doi.org/10.1111/j.1364-3703.2011.00783.x
99. Liu L, Zhang L, Wang Y, Zhan H, Yang J, Peng L, Yang L, He B, Lu B, Wang Y, Gao J, Hsiang T. 2020. Distribution, identification and characterization of *Colletotrichum lineola* and *C. panacicola* causing anthracnose on ginseng in northeast China. Crop Prot 137:105265. https://doi.org/10.1016/j.cropro.2020.105265
100. Liu L, Zhang L, Qiu P, Wang Y, Liu Y, Li Y, Gao J, Hsiang T. 2020. Leaf spot of *Polygonatum odoratum* caused by *Colletotrichum spaethianum*. J Gen Plant Pathol 86:157–161. https://doi.org/10.1007/s10327-019-00903-4
101. De Silva DD, Crous PW, Ades PK, Hyde KD, Taylor PWJ. 2017. Life styles of *Colletotrichum* species and implications for plant biosecurity. Fungal Biol Rev31:155–168. https://doi.org/10.1016/j.fbr.2017.05.001
102. O'Connell R, Herbert C, Sreenivasaprasad S, Khatib M, Esquerré-Tugayé M-T, Dumas B. 2004. A novel *Arabidopsis-Colletotrichum* pathosystem for the molecular dissection of plant-fungal interactions. Mol Plant Microbe Interact 17:272–282. https://doi.org/10.1094/MPMI.2004.17.3.272
103. O'Connell RJ, Thon MR, Hacquard S, Amyotte SG, Kleemann J, Torres MF, Damm U, Buiate EA, Epstein L, Alkan N, et al. 2012. Lifestyle transitions in plant pathogenic *Colletotrichum* fungi deciphered by genome and transcriptome analyses. Nat Genet 44:1060–1065. https://doi.org/10.1038/ng.2372
104. Zhdanova NN, Zakharchenko VA, Vember VV, Nakonechnaya LT. 2000. Fungi from Chernobyl: mycobiota of the inner regions of the containment structures of the damaged nuclear reactor. Mycol Res 104:1421–1426. https://doi.org/10.1017/S0953756200002756
105. Luo X-W, Gao C-H, Lu H-M, Wang J-M, Su Z-Q, Tao H-M, Zhou X-F, Yang B, Liu Y-H. 2020. HPLC-DAD-guided isolation of diversified chaetoglobosins from the coral-associated fungus *Chaetomium globosum* C2F17. Molecules 25:1237. https://doi.org/10.3390/molecules25051237
106. Qi J, Jiang L, Zhao P, Chen H, Jia X, Zhao L, Dai H, Hu J, Liu C, Shim SH, Xia X, Zhang L. 2020. Chaetoglobosins and azaphilones from *Chaetomium globosum* associated with Apostichopus japonicus. Appl Microbiol Biotechnol 104:1545–1553. https://doi.org/10.1007/s00253-019-10308-0
107. Gao W, He Y, Li F, Chai C, Zhang J, Guo J, Chen C, Wang J, Zhu H, Hu Z, Zhang Y. 2019. Antibacterial activity against drug-resistant microbial pathogens of cytochalasan alkaloids from the arthropod-associated fungus *Chaetomium globosum* TW1-1. Bioorg Chem 83:98–104. https://doi.org/10.1016/j.bioorg.2018.10.020
108. Kushmaro A, Rosenberg E, Fine M, Ben Haim Y, Loya Y. 1998. Effect of temperature on bleaching of the coral *Oculina patagonica* by *Vibrio* AK-1. Mar Ecol Prog Ser 171:131–137. https://doi.org/10.3354/meps171131
109. Mouchka ME, Hewson I, Harvell CD. 2010. Coral-associated bacterial assemblages: current knowledge and the potential for climate-driven impacts. Integr Comp Biol 50:662–674. https://doi.org/10.1093/icb/icq061
110. Xie H, Chen SL. 2009. Antioxidant activity of endophytic *Chaetomium globosum* from Eucommia ulmoides. Mygosystema 28:591–596.
111. Yakovleva I, Bhagooli R, Takemura A, Hidaka M. 2004. Differential susceptibility to oxidative stress of two scleractinian corals: antioxidant functioning of mycosporine-glycine. Comp Biochem Physiol B Biochem Mol Biol 139:721–730. https://doi.org/10.1016/j.cbpc.2004.08.016
112. Wang W, Lin Y, Teng F, Ji D, Xu Y, Chen C, Xie C. 2018. Comparative transcriptome analysis between heat-tolerant and sensitive *Pyropia haitanensis* strains in response to high temperature stress. Algal Research 29:104–112. https://doi.org/10.1016/j.algal.2017.11.026
113. Yu X, Yu K, Huang W, Liang J, Qin Z, Chen B, Yao Q, Liao Z. 2020. Thermal acclimation increases heat tolerance of the scleractinian coral *Acropora pruinosa*. Sci Total Environ 733:139319. https://doi.org/10.1016/j.scitotenv.2020.139319
114. Liu X, Huang X, Chu C, Xu H, Wang L, Xue Y, Arifeen Muhammad ZU, Inagaki F, Liu C. 2022. Genome, genetic evolution, and environmental adaptation mechanisms of *Schizophyllum commune* in deep subseafloor coal-bearing sediments. iScience 25:104417. https://doi.org/10.1016/j.isci.2022.104417
115. Xu W, Guo S, Gong L, Alias SA, Pang K-L, Luo Z-H. 2018. Phylogenetic survey and antimicrobial activity of cultivable fungi associated with five scleractinian coral species in the South China Sea. Botanica Marina 61:75–84. https://doi.org/10.1515/bot-2017-0005
116. Wang W, Li Q, Lai Q, Lin Y, Zhang Q, Chen J. 2021. Screening of anti - *Vibrio* activity of marine fungal methanolic fractions to control vibriosis in white shrimp (*Litopenaeus vannamei*). Aquac Res52:5517–5526. https://doi.org/10.1111/are.15425
117. Fabina NS, Putnam HM, Franklin EC, Stat M, Gates RD. 2013. Symbiotic specificity, association patterns, and function determine community responses to global changes: defining critical research areas for coral - *Symbiodinium* symbioses. Glob Chang Biol 19:3306–3316. https://doi.org/10.1111/gcb.12320
118. Baker DM, Freeman CJ, Wong JCY, Fogel ML, Knowlton N. 2018. Climate change promotes parasitism in a coral symbiosis. ISME J 12:921–930. https://doi.org/10.1038/s41396-018-0046-8
119. Ng TY, Ang P. 2016. Low symbiont diversity as a potential adaptive strategy in a marginal non-reefal environment: a case study of corals in Hong Kong. Coral Reefs 35:941–957. https://doi.org/10.1007/s00338-016-1458-4
120. Lee MJ, Jeong HJ, Jang SH, Lee SY, Kang NS, Lee KH, Kim HS, Wham DC, LaJeunesse TC. 2016. Most low-abundance "background" *Symbiodinium* spp. are transitory and have minimal functional significance for symbiotic corals. Microb Ecol 71:771–783. https://doi.org/10.1007/s00248-015-0724-2
121. Ziegler M, Arif C, Burt JA, Dobretsov S, Roder C, LaJeunesse TC, Voolstra CR. 2017. Biogeography and molecular diversity of coral symbionts in the genus *Symbiodinium* around the Arabian Peninsula. J Biogeogr 44:674–686. https://doi.org/10.1111/jbi.12913
122. Howells EJ, Bauman AG, Vaughan GO, Hume BCC, Voolstra CR, Burt JA. 2020. Corals in the hottest reefs in the world exhibit symbiont fidelity not flexibility. Mol Ecol 29:899–911. https://doi.org/10.1111/mec.15372
123. Hume BCC, Mejia-Restrepo A, Voolstra CR, Berumen ML. 2020. Fine-scale delineation of Symbiodiniaceae genotypes on a previously bleached central Red Sea reef system demonstrates a prevalence of coral host-specific associations. Coral Reefs 39:583–601. https://doi.org/10.1007/s00338-020-01917-7
124. Deng Y, Jiang Y-H, Yang Y, He Z, Luo F, Zhou J. 2012. Molecular ecological network analyses. BMC Bioinformatics 13:113. https://doi.org/10.1186/1471-2105-13-113
125. Ma B, Wang H, Dsouza M, Lou J, He Y, Dai Z, Brookes PC, Xu J, Gilbert JA. 2016. Geographic patterns of co-occurrence network topological features for soil microbiota at continental scale in eastern China. ISME J 10:1891–1901. https://doi.org/10.1038/ismej.2015.261
126. Jiao C, Zhao D, Zeng J, Guo L, Yu Z. 2020. Disentangling the seasonal co-occurrence patterns and ecological stochasticity of planktonic and benthic bacterial communities within multiple lakes. Sci Total Environ 740:140010. https://doi.org/10.1016/j.scitotenv.2020.140010
127. Yuan MM, Guo X, Wu L, Zhang YA, Xiao N, Ning D, Shi Z, Zhou X, Wu L, Yang Y, Tiedje JM, Zhou J. 2021. Climate warming enhances microbial network complexity and stability. Nat Clim Chang 11:343–348. https://doi.org/10.1038/s41558-021-00989-9
128. Liu S, Yu H, Yu Y, Huang J, Zhou Z, Zeng J, Chen P, Xiao F, He Z, Yan Q. 2022. Ecological stability of microbial communities in Lake Donghu regulated by keystone taxa. Ecol Indic136:108695. https://doi.org/10.1016/j.ecolind.2022.108695

129. Ramayo-Caldas Y, Mach N, Lepage P, Levenez F, Denis C, Lemonnier G, Leplat J-J, Billon Y, Berri M, Doré J, Rogel-Gaillard C, Estellé J. 2016. Phylogenetic network analysis applied to pig gut microbiota identifies an ecosystem structure linked with growth traits. ISME J 10:2973–2977. https://doi.org/10.1038/ismej.2016.77
130. Wagg C, Schlaeppi K, Banerjee S, Kuramae EE, van der Heijden MGA. 2019. Fungal-bacterial diversity and microbiome complexity predict ecosystem functioning. Nat Commun 10:4841. https://doi.org/10.1038/s41467-019-12798-y
131. Han Q, Ma Q, Chen Y, Tian B, Xu L, Bai Y, Chen W, Li X. 2020. Variation in rhizosphere microbial communities and its association with the symbiotic efficiency of rhizobia in soybean. ISME J 14:1915–1928. https://doi.org/10.1038/s41396-020-0648-9
132. Lima LFO, Weissman M, Reed M, Papudeshi B, Alker AT, Morris MM, Edwards RA, de Putron SJ, Vaidya NK, Dinsdale EA, Medina M, McFall-Ngai MJ. 2020. Modeling of the coral microbiome: the influence of temperature and microbial network. mBio 11:10–1128. https://doi.org/10.1128/mBio.02691-19
133. Leite DCA, Salles JF, Calderon EN, Castro CB, Bianchini A, Marques JA, van Elsas JD, Peixoto RS. 2018. Coral bacterial-core abundance and network complexity as proxies for anthropogenic pollution. Front Microbiol 9:833. https://doi.org/10.3389/fmicb.2018.00833
134. Zhu W, Liu X, Zhu M, Xia J, Chen R, Li X. 2023. Coastal upwelling under anthropogenic influence drives the community change, assembly process, and co‐occurrence pattern of coral associated microorganisms. J Geophys Res Oceans 128. https://doi.org/10.1029/-2022JC019307
135. Estrada-Peña A, Cabezas-Cruz A, Pollet T, Vayssier-Taussat M, Cosson J-F. 2018. High throughput sequencing and network analysis disentangle the microbial communities of ticks and hosts within and between ecosystems. Front Cell Infect Microbiol 8:236. https://doi.org/10.3389/fcimb.2018.00236
136. Liu B, Guan L, Chen H. 2021. Detecting 2020 coral bleaching event in the Northwest Hainan Island using CoralTemp SST and sentinel-2B MSI imagery. Remote Sens 13:4948. https://doi.org/10.3390/rs13234948
137. Mo S, Chen T, Chen Z, Zhang W, Li S. 2022. Marine heatwaves impair the thermal refugia potential of marginal reefs in the northern South China Sea. Sci Total Environ 825:154100. https://doi.org/10.1016/j.scitotenv.2022.154100
138. Zhao W, Chen L, Liu M, Huang K, Ding Y, Xiao J, Tian P, Liu J, Zhang X-H, Niu W, Wang X, Biddle JF. 2023. Sedimentary *Vibrio* blooms in the Xisha Islands may associate with the 2020 coral bleaching event. Appl Environ Microbiol 89:e0054323. https://doi.org/10.1128/aem.00543-23
139. English S, Wilkinson C, Baker V. 1994. Survey manual for tropical marine resources. Australian Institute of Marine Science, Townsville.
140. Xiao J, Wang W, Wang X, Tian P, Niu W. 2022. Recent deterioration of coral reefs in the South China Sea due to multiple disturbances. PeerJ 10:e13634. https://doi.org/10.7717/peerj.13634
141. Lang S. 2022. The status and cause analysis of coral bleaching in Hainan Island and Xisha Islands. Hainan Tropical Ocean University
142. Veron JEN. 2000. Coral of the World. Australian Institute of Marine Science, Townsville.
143. Huang H. 2018. Coral reef atlas of Xisha Islands. Science Press, Beijing.
144. Lajeunesse TC, Trench RK. 2000. Biogeography of two species of *Symbiodinium* (Freudenthal) inhabiting the intertidal sea anemone Anthopleura elegantissima (Brandt). Biol Bull 199:126–134. https://doi.org/10.2307/1542872
145. Gaither MR, Szabó Z, Crepeau MW, Bird CE, Toonen RJ. 2011. Preservation of corals in salt-saturated DMSO buffer is superior to ethanol for PCR experiments. Coral Reefs 30:329–333. https://doi.org/10.1007/s00338-010-0687-1
146. Coleman AW, Suarez A, Goff LJ. 1994. Molecular delineation of species and syngens in volvocacean green algae (chlorophyta)[1]. J Phycol30:80–90. https://doi.org/10.1111/j.0022-3646.1994.00080.x
147. Toju H, Tanabe AS, Yamamoto S, Sato H, Lespinet O. 2012. High-coverage ITS primers for the DNA-based identification of ascomycetes and basidiomycetes in environmental samples. PLoS One 7:e40863. https://doi.org/10.1371/journal.pone.0040863
148. Bolyen E, Rideout JR, Dillon MR, Bokulich NA, Abnet CC, Al-Ghalith GA, Alexander H, Alm EJ, Arumugam M, Asnicar F, et al. 2019. Reproducible, interactive, scalable and extensible microbiome data science using QIIME 2. Nat Biotechnol 37:852–857. https://doi.org/10.1038/s41587-019-0209-9
149. Callahan BJ, McMurdie PJ, Rosen MJ, Han AW, Johnson AJA, Holmes SP. 2016. DADA2: high-resolution sample inference from Illumina amplicon data. Nat Methods 13:581–583. https://doi.org/10.1038/nmeth.3869
150. Thornhill DJ, Lajeunesse TC, Santos SR. 2007. Measuring rDNA diversity in eukaryotic microbial systems: how intragenomic variation, pseudogenes, and PCR artifacts confound biodiversity estimates. Mol Ecol 16:5326–5340. https://doi.org/10.1111/j.1365-294X.2007.03576.x
151. Stat M, Bird CE, Pochon X, Chasqui L, Chauka LJ, Concepcion GT, Logan D, Takabayashi M, Toonen RJ, Gates RD. 2011. Variation in *Symbiodinium* ITS2 sequence assemblages among coral colonies. PLoS One 6:e15854. https://doi.org/10.1371/journal.pone.0015854
152. Cunning R, Gates RD, Edmunds PJ. 2017. Using high-throughput sequencing of ITS2 to describe *Symbiodinium* metacommunities in St. John, US Virgin Islands. PeerJ 5:e3472. https://doi.org/10.7717/peerj.3472
153. Howe-Kerr LI, Bachelot B, Wright RM, Kenkel CD, Bay LK, Correa AMS. 2020. Symbiont community diversity is more variable in corals that respond poorly to stress. Glob Chang Biol 26:2220–2234. https://doi.org/10.1111/gcb.14999
154. Nilsson RH, Larsson K-H, Taylor AFS, Bengtsson-Palme J, Jeppesen TS, Schigel D, Kennedy P, Picard K, Glöckner FO, Tedersoo L, Saar I, Kõljalg U, Abarenkov K. 2019. The UNITE database for molecular identification of fungi: handling dark taxa and parallel taxonomic classifications. Nucleic Acids Res 47:D259–D264. https://doi.org/10.1093/nar/gky1022
155. Oksanen J, Simpson GL, Blanchet FG, Kindt R, Legendre P, Minchin PR, O'Hara RH, Solymos P, Stevens MHM, Szoecs E, et al. 2015. Vegan: community ecology package. R Package version 2.3-0
156. De Cáceres M, Legendre P. 2009. Associations between species and groups of sites: indices and statistical inference. Ecology 90:3566–3574. https://doi.org/10.1890/08-1823.1
157. Glasl B, Bourne DG, Frade PR, Thomas T, Schaffelke B, Webster NS. 2019. Microbial indicators of environmental perturbations in coral reef ecosystems. Microbiome 7:94. https://doi.org/10.1186/s40168-019-0705-7
158. Nguyen NH, Song Z, Bates ST, Branco S, Tedersoo L, Menke J, Schilling JS, Kennedy PG. 2016. FUNGuild: an open annotation tool for parsing fungal community datasets by ecological guild. Fungal Ecol20:241–248. https://doi.org/10.1016/j.funeco.2015.06.006
159. Shannon P, Markiel A, Ozier O, Baliga NS, Wang JT, Ramage D, Amin N, Schwikowski B, Ideker T. 2003. Cytoscape: a software environment for integrated models of biomolecular interaction networks. Genome Res 13:2498–2504. https://doi.org/10.1101/gr.1239303
160. Faust K, Raes J. 2012. Microbial interactions: from networks to models. Nat Rev Microbiol 10:538–550. https://doi.org/10.1038/nrmicro2832
161. Brown MB. 1975. 400: a method for combining non-independent, one-sided tests of significance. Biometrics 31:987. https://doi.org/10.2307/2529826
162. Benjamini Y, Hochberg Y. 1995. Controlling the false discovery rate: a practical and powerful approach to multiple testing. J R Stat Soc Series B Stat Methodol 57:289–300. https://doi.org/10.1111/j.2517-6161.1995.tb02031.x
163. Zhang B, Ning D, Yang Y, Van Nostrand JD, Zhou J, Wen X. 2020. Biodegradability of wastewater determines microbial assembly mechanisms in full-scale wastewater treatment plants. Water Res 169:115276. https://doi.org/10.1016/j.watres.2019.115276
164. Edwards J, Johnson C, Santos-Medellín C, Lurie E, Podishetty NK, Bhatnagar S, Eisen JA, Sundaresan V. 2015. Structure, variation, and assembly of the root-associated microbiomes of rice. Proc Natl Acad Sci U S A 112:E911–E920. https://doi.org/10.1073/pnas.1414592112
165. Freeman LC. 1977. A set of measures of centrality based on betweenness. Sociometry 40:35. https://doi.org/10.2307/3033543